華中師範大學
CENTRAL CHINA NORMAL UNIVERSITY

缪原子精密谱中的核结构效应计算

Precision Calculation of Nuclear Structure Effects in Muonic Atom

计晨

华中师范大学 粒子物理研究所

粒子与核物理理论冬季研讨班
2022年12月28日

The proton radius puzzle

- electron-proton experiments: $r_p = 0.8751(61)$ fm
  - eH spectroscopy
  - $e{-}p$ scattering
- muon-proton experiments: $r_p = 0.8409(4)$ fm
  - μH Lamb shift (E_{2S-2P}) [PSI-CREMA]

  Pohl *et al.*, Nature (2010); Antognini *et al.*, Science (2013)

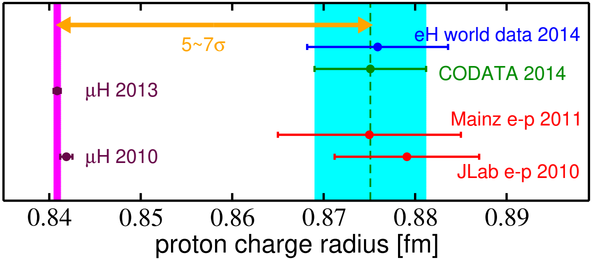

Origin of the discrepancy?

- Search for the origin of the radius puzzle
  - Lepton universality violation?
  - Exotic hadron structure?
  - Under-estimated experimental uncertainties in eH and e-p?

These explanations are still in debate...

Lepton universality violation?

Physics beyond standard model

- new force carrier, e.g., dark photon: couples differently with e and μ
- explain both the r_p puzzle & $(g-2)_\mu$ puzzle

Tucker-Smith, Yavin, PRD 83 (2011) 101702
Batell, McKeen, Pospelov, PRL 107 (2011) 011803
Barger, Chiang, Keung, Marfatia, PRL 106 (2011) 153001
Endo, Hamaguchi, Mishima, PRD 86 (2012) 095029

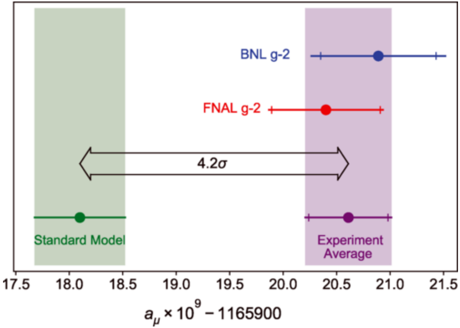

$(g-2)_\mu$ collaboration, PRL 126 (2021) 141801

Error in ep scattering experiment (analysis)?

- $G_E^p(Q^2) = 1 - \frac{1}{6}\, \boldsymbol{r_p^2}\, Q^2 + \ldots$
- Q^2 not small enough / floating normalization

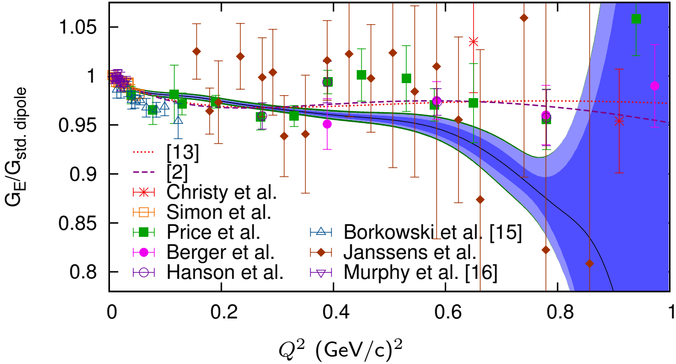

- dispersion analysis on n/p EM form factors: $r_p = 0.84(1)$ fm

Lorenz, Hammer, Meißner, EPJA 48 (2012) 151

Lorenz, Hammer, Meißner, Dong, PRD 91 (2015) 014023

- deficiency in radiative correction model:

Lee, Arrington, Hill, PRD 92 (2015) 013013

Underestimated uncertainties in eH spectroscopies?

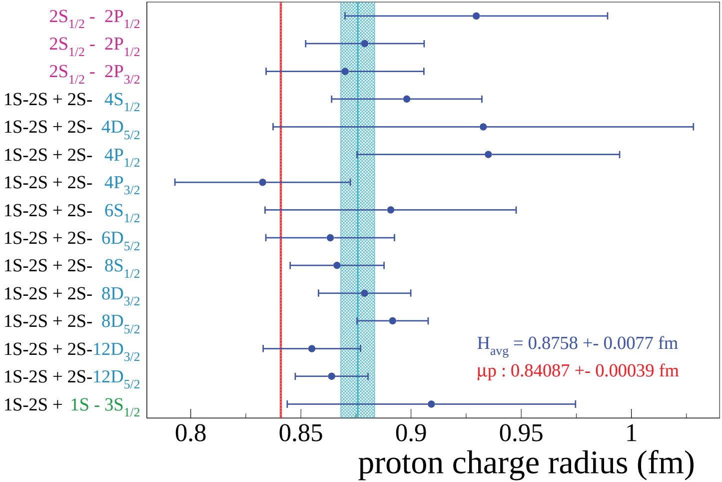

Phol *et al.*, Annu. Rev. Nucl. Part. Sci 63 (2013) 175

- large uncertainty in individual eH measurement
- correlated measurements?

To understand the radius puzzle

- New experiments to solve the puzzle
  - eH spectroscopy (MPQ, LKB, York U.)
  - ep scattering (JLab, Mainz, Tohoku U.)
  - μp scattering (PSI-MUSE)

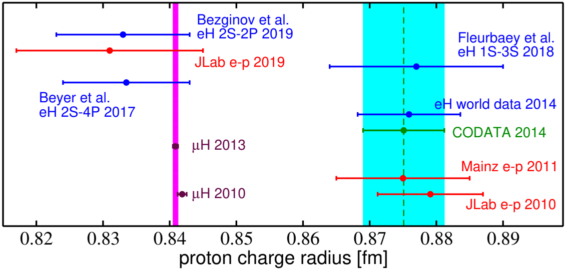

The radius puzzle is nearly but not fully solved

Explore radius puzzle in other nuclei

- Lamb shift measurements in light muonic atoms (PSI-CREMA)
  - $\mu^2\mathrm{H}$ [Pohl *et al.*, Science 2016]
  - $\mu^4\mathrm{He}^+$ [Krauth *et al.*, Nature 2021]
  - $\mu^3\mathrm{He}^+$ [measured in 2014, finalizing analyses]
  - $\mu^3\mathrm{H}$, $\mu\mathrm{Li}$, $\mu\mathrm{Be}$ [in progress]

Extract nuclear electric radii from spectroscopy

- Hyperfine splittings measurements in light muonic atoms (PSI-CREMA)
  - $\mu^2\mathrm{H}$, $\mu^3\mathrm{He}^+$ [in plan]

Extract nuclear magnetic radii from spectroscopy

- $e^{3,4}\mathrm{He}$ spectroscopies

determine $^3\mathrm{He}$-$^4\mathrm{He}$ charge radius isotope shift

- $e^{6,7}\mathrm{Li}$ hyperfine structures

determine $^{6,7}\mathrm{Li}$ magnetic Zemach radius

Electron scattering and nuclear structures

- Traditional nuclear theory is based on independent particle models (IPM)
- IPM poorly describes short-range nucleon-nucleon correlation and exotic nuclear structure
- Electron Scattering (ES) provides a clean way to probe nuclear structure and spectrum
- Precise Electromagnetic probes give accurate constraints on nucleon-nucleon interaction and meson-exchange current

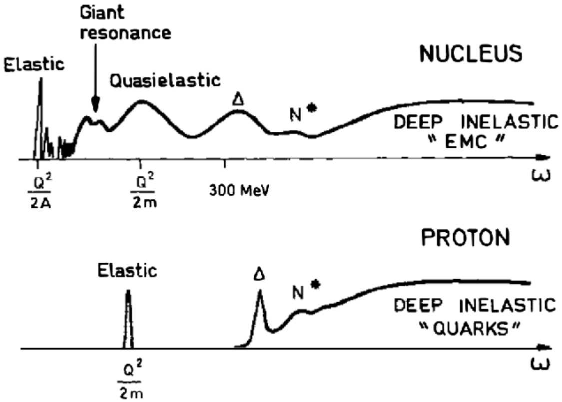

Elastic electron scattering and nuclear form factors

- Elastic electron-nucleus scattering provides information on nuclear charge, quadrupole, magnetic structures

$$\frac{d\sigma(E,\theta)}{d\Omega}^{PWIA} = \sigma_{Mott}(E,\theta)[A(q) + B(q)tan(\theta/2)^2]$$

$$A(q) = F_{C0}(q)^2 + (M_d^2 Q_d)^2 \frac{8}{9}\eta^2 F_{C2}^2(q) + (\frac{M_d}{M_p}\mu_d)^2 \frac{2}{3}\eta(1+\eta) F_{M1}^2(q)$$

$$B(q) = (\frac{M_d}{M_p}\mu_d)^2 \frac{4}{3}\eta(1+\eta)^2 F_{M1}^2(q) \qquad \eta = q^2/(4M_d^2)$$

- scattering on light nuclei were intensively studied during 1960-1980
- Most recent measurements were done at Jefferson Lab and Mainz Microtron (light stable nuclei)

Reviews:
Frois, Papanicolas, Ann. Rev. Nucl. Part. Sci. 37, 133 (1987)
Hofstadter, Rev. Mod. Phys. 28, 214 (1956)
Sick, Prog. Part. Nucl. Phys. 47, 245 (2001); arXiv:1505.06924

New electron scattering experimental plan

- JLab & Mainz: measure G_E and G_M for light nuclei at low Q^2
  - ep scattering (JLab PRad: Xiong et al., Nature 575, 147 (2019)
  - $e-^2$H scattering (JLab DRad: improve precision by a factor of 2)
  - $e-^3$H & e^3He scattering

Experiments Proposal:
Mainz A1: wwwa1.kph.uni-mainz.de/experiments-and-accepted-proposals/
JLab Hall A: www.jlab.org/physics/experiments

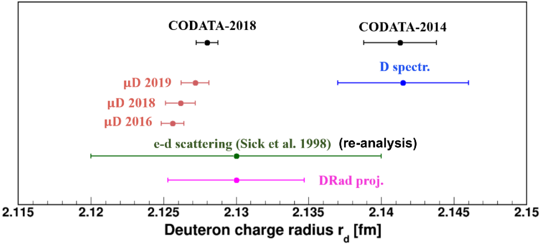

New electron scattering experimental plan

- JLab & Mainz: measure G_E and G_M for light nuclei at low Q^2
  - ep scattering (JLab PRad: Xiong et al., Nature 575, 147 (2019)
  - $e-^2$H scattering (JLab DRad: improve precision by a factor of 2)
  - $e-^3$H & e^3He scattering

Experiments Proposal:
Mainz A1: wwwa1.kph.uni-mainz.de/experiments-and-accepted-proposals/
JLab Hall A: www.jlab.org/physics/experiments

- SCRIT (RIKEN) & ELISe (GSI-FAIR): electron scattering on exotic nuclei

Suda, Wakasugi, Prog. Part. Nucl. Phys 55, 417 (2005)

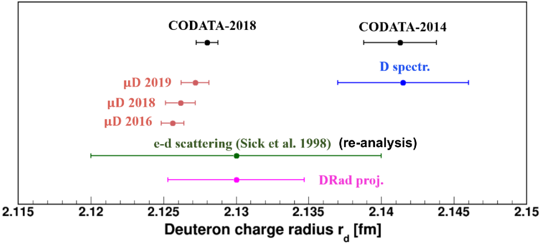

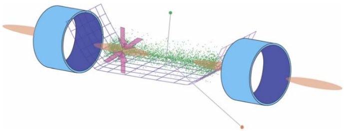

Laser spectroscopy of radioactive isotopes

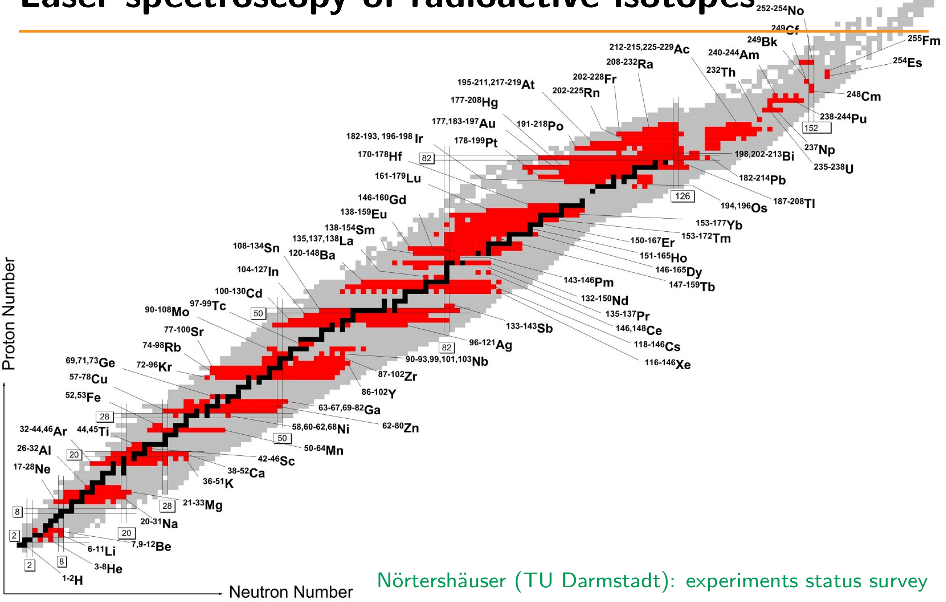

Nörtershäuser (TU Darmstadt): experiments status survey

Laser spectroscopy of radioactive isotopes

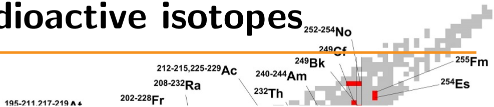

light exotic nuclei:

Laser Spectroscopic Determination of the ^{6}He Nuclear Charge Radius

L.-B. Wang, P. Mueller, K. Bailey, G. W. F. Drake, J. P. Greene, D. Henderson, R. J. Holt, R. V. F. Janssens, C. L. Jiang, Z.-T. Lu, T. P. O'Connor, R. C. Pardo, K. E. Rehm, J. P. Schiffer, and X. D. Tang

Phys. Rev. Lett. **93**, 142501 – Published 27 September 2004

Nuclear Charge Radius of ^{8}He

P. Mueller, I. A. Sulai, A. C. C. Villari, J. A. Alcántara-Núñez, R. Alves-Condé, K. Bailey, G. W. F. Drake, M. Dubois, C. Eléon, G. Gaubert, R. J. Holt, R. V. F. Janssens, N. Lecesne, Z.-T. Lu, T. P. O'Connor, M.-G. Saint-Laurent, J.-C. Thomas, and L.-B. Wang

Phys. Rev. Lett. **99**, 252501 – Published 21 December 2007

Charge radii and ground state structure of lithium isotopes: Experiment and theory reexamined

W. Nörtershäuser, T. Neff, R. Sánchez, and I. Sick

Phys. Rev. C **84**, 024307 – Published 10 August 2011

Nuclear Charge Radii of ^{7,9,10}Be and the One-Neutron Halo Nucleus ^{11}Be

W. Nörtershäuser, D. Tiedemann, M. Žáková, Z. Andjelkovic, K. Blaum, M. L. Bissell, R. Cazan, G. W. F. Drake, Ch. Geppert, M. Kowalska, J. Krämer, A. Krieger, R. Neugart, R. Sánchez, F. Schmidt-Kaler, Z.-C. Yan, D. T. Yordanov, and C. Zimmermann

Phys. Rev. Lett. **102**, 062503 – Published 13 February 2009

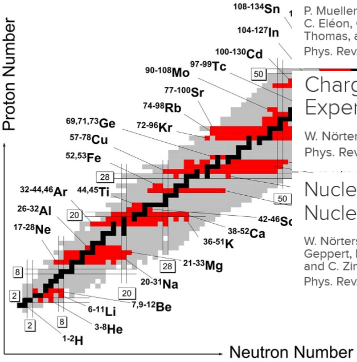

Nörtershäuser (TU Darmstadt): experiments status survey

Theoretical studies of nuclear structure

- Nuclear theory has made great progress in the past 30 years
- microscopic nucelon-nucleon interaction development
- microscopic nucleon electroweak interaction development
- quantum many-body calculations (ab initio) make accurate study of nuclear structure and reaction possible
- Recent development can make rigorous uncertainty quantification in theoretical predictions

Phenomenological potential

- **Argonne v_{18}** fitted to
  - 1787 pp & 2514 np observables for $E_{lab} \leq 350$ MeV with $\chi^2/\mathrm{datum} = 1.1$
  - nn scattering length & ^{2}H binding energy

- **Urbana IX**

  $$V_{ijk} = V_{ijk}^{2\pi P} + V_{ijk}^{R}$$

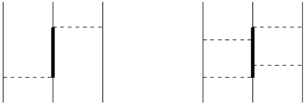

Phenomenological potentials

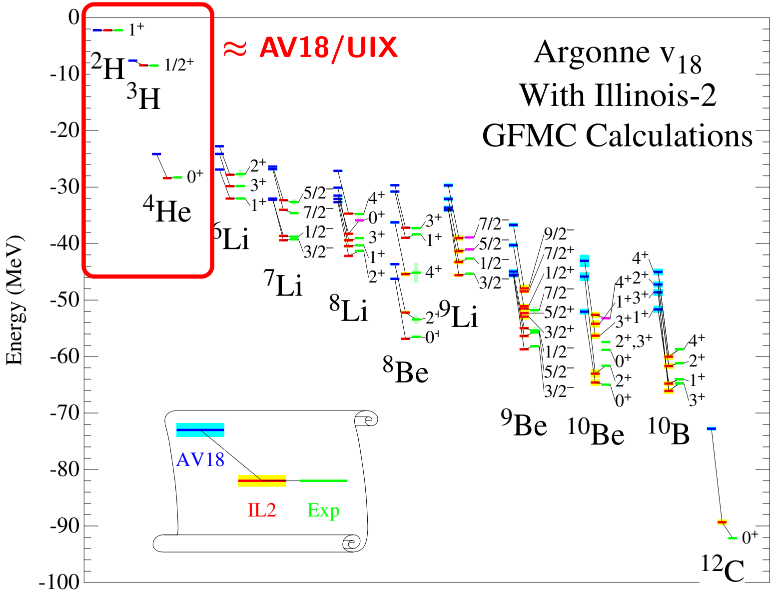

Chiral effective field theory potential

- **effective theory**
  of low-energy QCD

- **nuclear forces**
  are built in systematic
  expansions of Q/Λ_χ

- **coupling constants**
  fitted to nuclear data

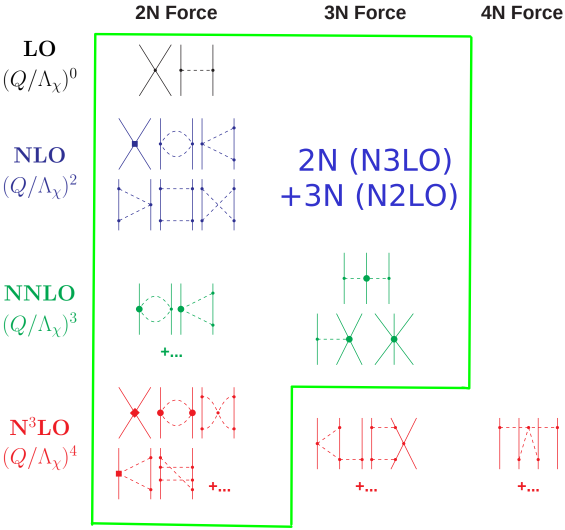

Chiral effective field theory potential

- Chiral EFT determination of nuclear binding energies and charge radii

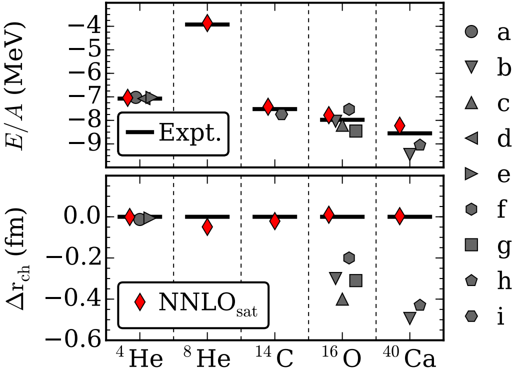

Ekström et al., Phys. Rev. C 91, 051301 (2015)

Progress in ab initio nuclear structure theories

- Advances in ab initio calculations made nuclear chart accessible

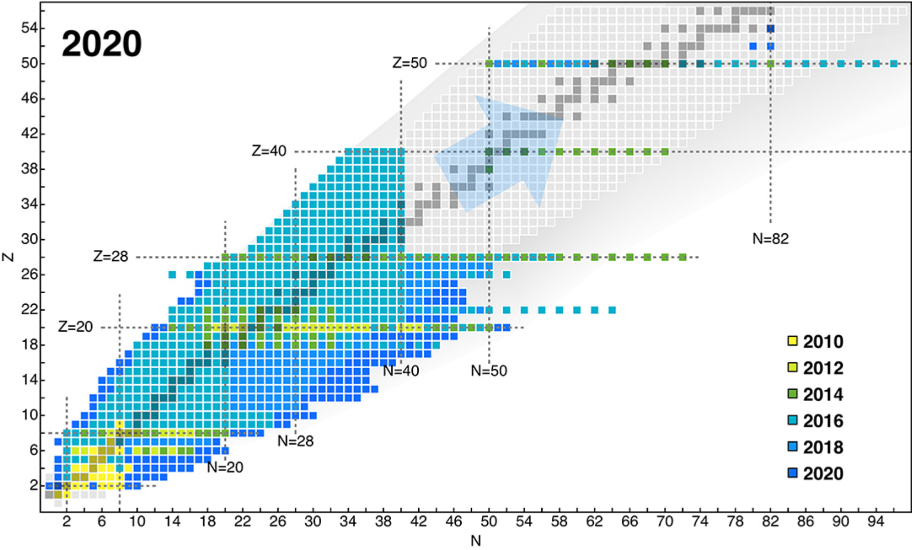

Hergert, Front. Phys. 8, 379 (2020)

Current understanding of nuclear structure

- Both experiments and theories have made great progress in understanding nuclear structures
- However, discrepancies appear at precision levels
  - discrepancies among experiments
  - disagreement between experiments and theories
  - theories face challenges in accurately describing exotic structures

The ^{2}H radius puzzle

- μ^2H Lamb shift: $r_d = 2.12562(78)$ fm   Pohl, *et al.*, Science 353, 669 (2016)
- CODATA-2014: $r_d = 2.1415(45)$ fm

- isotope shift $r_d^2 - r_p^2$:
  $\delta(\mu^2\mathrm{H}, \mu\mathrm{H}) = 3.8112(34)$ fm^2
  $\delta(e^2\mathrm{H}, e\mathrm{H}) = 3.8201(07)$ fm^2 Parthey, *et al.*, PRL (2010)

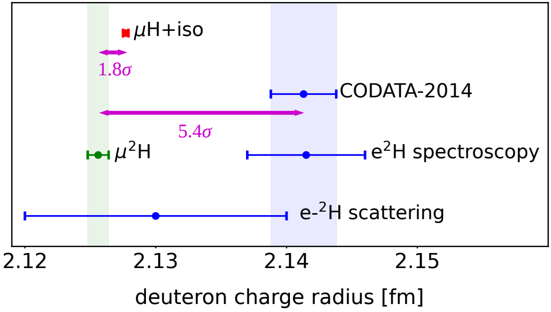

^{2}H charge & magnetic form factors

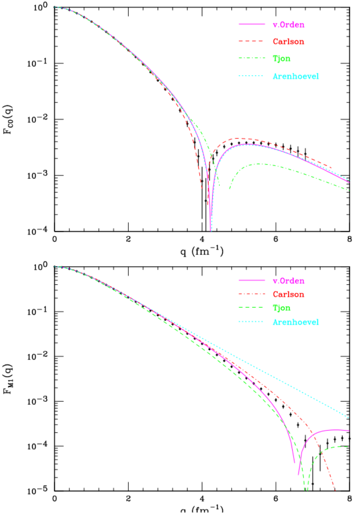

- ^{2}H $G_C(q)$:
  better agreement between theory & data
- ^{2}H $G_M(q)$:
  less agreement between theory & data

Sick, arXiv:1505.06924

The helium isotope shift puzzle

- Discrepancies in ^{3}He-^{4}He charge radius isotope shift measurements

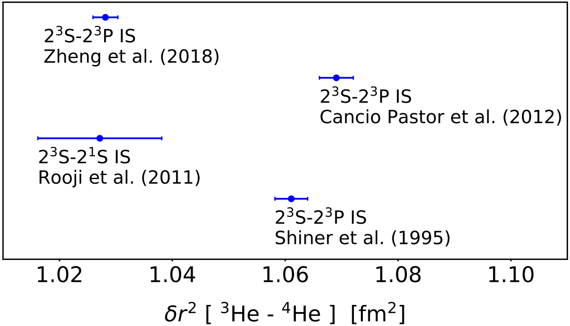

Zheng, et al., Phys. Rev. Lett. 119, 263002 (2017)
Cancio Pastor, et al., Phys. Rev. Lett. 108, 143001 (2012)
van Rooij, et al., Science 333, 196 (2011)
Shiner, et al. Phys. Rev. Lett. 74, 3553 (1995)

^{3}He charge & magnetic form factors

- ^{3}H $G_C(q)$:
  better agreement between theory & data
- ^{3}H $G_M(q)$:
  less agreement between theory & data

Sick, arXiv:1505.06924

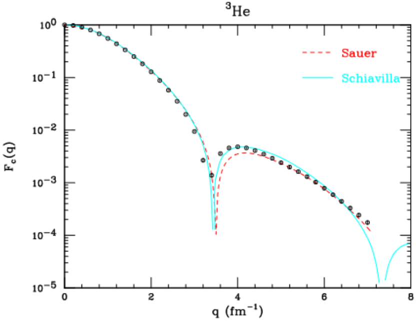

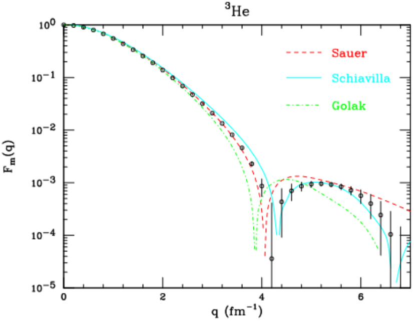

Spectroscopy and charge radii of ^{6,8}He

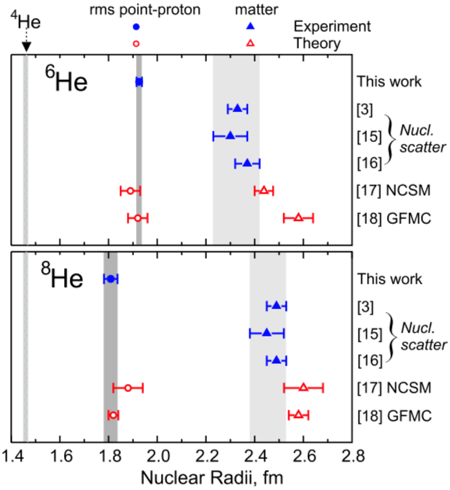

- difference between experiments and theories indicate discrepancies in the description of halo structures in ^{6,8}He

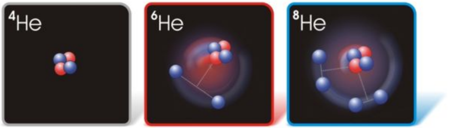

Wang et al., Phys. Rev. Lett. 93, 142501 (2004)
Muller et al., Phys. Rev. Lett. 99, 252501 (2007)

The lithium magnetic Zemach radius puzzle

- magnetic Zemach radius indicates nuclear magnetic distribution
- R_z discrepancies in spectroscopy and scattering experiments

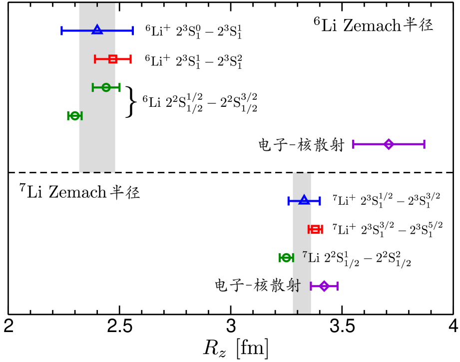

Puchalski, Pachucki, PRL 111, 243001 (2013)
Qi et al., PRL 125, 183002 (2020)
Li et al., PRL 124, 063002 (2020)
Guan et al., PRA 102, 030801(R) (2020)

Spectroscopy and Li isotopes charge radii

- cluster configuration in ^{6,7}Li
- halo structures in ^{11}Li
- disagreement between ab initio theory and data

TRIUMF & GSI:
Phys. Rev. Lett. 93, 113002 (2004); Phys. Rev. C 84, 024307 (2011);
Phys. Rev. A 83, 012516 (2011)

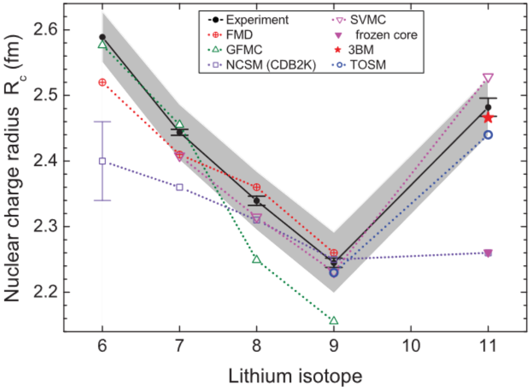

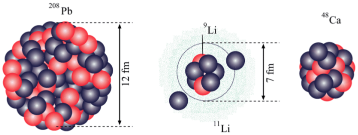

Challenges in nuclear structure studies

- precision spectroscopy brings nuclear structure study into precision era
- electromagnetic probes provides important information to improve nuclear potentials and ab initio theories

μH Lamb shift experiment

Lamb Shift: 2S-2P splitting in atomic spectrum   Pic: Pohl *et al.* Nature (2010)

- **prompt X-ray ($t \sim 0$s):** μ^- stopped in H_2 gases

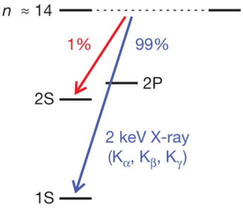

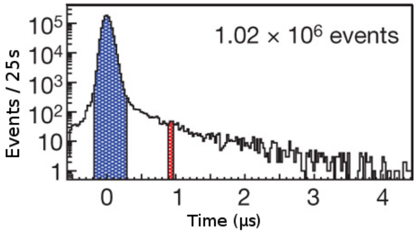

μH Lamb shift experiment

Lamb Shift: 2S-2P splitting in atomic spectrum — Pic: Pohl *et al.* Nature (2010)

- **prompt X-ray ($t \sim 0$s):** μ^- stopped in H_2 gases

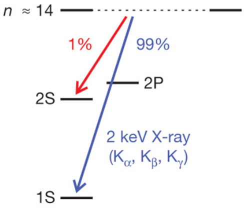

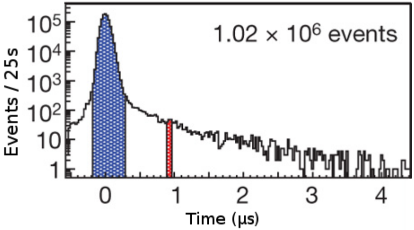

- **delayed X-ray ($t \sim 1\mu$s):** laser induced 2S→2P

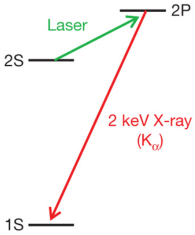

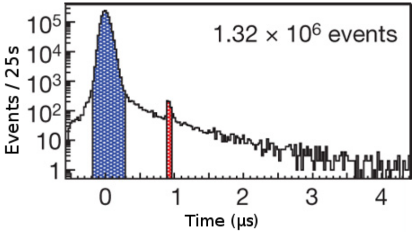

μH Lamb shift experiment

- measure $K_\alpha^{\text{delayed}} / K_\alpha^{\text{prompt}}$
- $\delta E_{LS} = h f_{res}$

Pic: Pohl *et al.* Nature (2010)

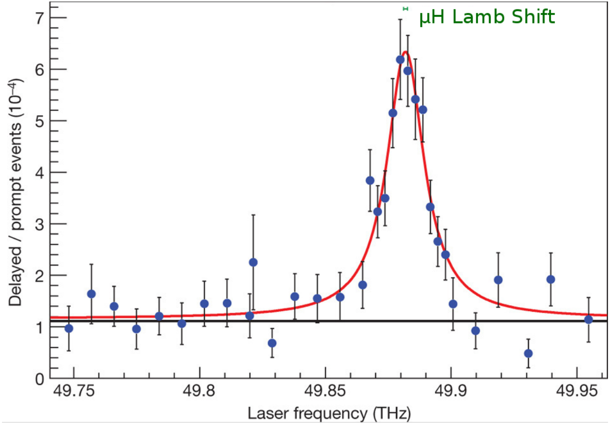

Lamb Shift & QED

- **Dirac theory:** $2s_{1/2}$ & $2p_{1/2}$ levels of hydrogen are degenerate
- **Lamb & Retherford Experiments (1947):**

$$\delta E_{LS} = E(2s_{1/2}) - E(2p_{1/2}) = 1057.8(1)\ \mathrm{MHz}$$

PHYSICAL REVIEW VOLUME 72, NUMBER 3 AUGUST 1, 1947

Fine Structure of the Hydrogen Atom by a Microwave Method* **

WILLIS E. LAMB, JR. AND ROBERT C. RETHERFORD
Columbia Radiation Laboratory, Department of Physics, Columbia University, New York, New York
(Received June 18, 1947)

- **Lamb shift gave the main impetus to the development of modern QED.**
- **Bethe Theory (1947):**
  - combine non-relativistic QM, 2nd order perturbation theory, & Kramers' QED renormalization concept
  - calculate the QED self-energy correction to account for Lamb's discovery

PHYSICAL REVIEW VOLUME 72, NUMBER 4 AUGUST 15, 1947

The Electromagnetic Shift of Energy Levels

H. A. BETHE
Cornell University, Ithaca, New York
(Received June 27, 1947)

BY very beautiful experiments, Lamb and Retherford[1] have shown that the fine struc- explained by a nuclear interaction of reasonable magnitude, and Uehling[5] has investigated the

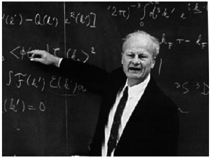

Radiative Correction at $\mathcal{O}(e^4)$ in QED

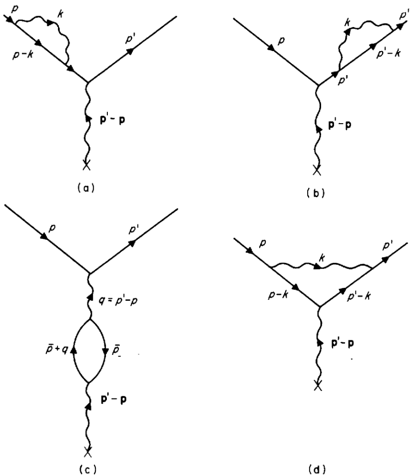

Fig. 9.2. The four contributions to the second-order radiative corrections to electron scattering.

Mandl, Shaw, Quantum Field Theory;
Aitchison, Hey, Gauge Theories in Particle Physics

- **(a,b) electron self-energy**

$$-\mathrm{i}\Sigma^{[2]}(p) = (-\mathrm{i}e)^2 \int \gamma^\nu \frac{-\mathrm{i}g_{\mu\nu}}{k^2} \frac{\mathrm{i}}{\not{p} - \not{k} - m} \gamma^\mu \frac{\mathrm{d}^4 k}{(2\pi)^4}$$

  - $\Sigma^{[2]}(\not{p} = m)$ and $\left.\frac{\mathrm{d}\Sigma^{[2]}}{\mathrm{d}\not{p}}\right|_{\not{p}=m}$ is **logarithmic** divergence at $k \to \infty$
  - **Renormalize:** electron field strength and electron mass

$$Z_2 = 1 + \left.\frac{\mathrm{d}\Sigma^{[2]}}{\mathrm{d}\not{p}}\right|_{\not{p}=m} \qquad m_0 - m = -Z_2^{-1}\Sigma^{[2]}(\not{p} = m)$$

- **(c) photon self-energy (vacuum polarization)**

$$\mathrm{i}\Pi_{\mu\nu}^{[2]}(q) = (-1)(-\mathrm{i}e)^2 \,\mathrm{Tr} \int \frac{\mathrm{d}^4 k}{(2\pi)^4} \frac{\mathrm{i}}{\not{q} + \not{k} - m} \gamma_\mu \frac{\mathrm{i}}{\not{k} - m} \gamma_\nu$$

$$= -e^2 \int \frac{\mathrm{d}^4 k}{(2\pi)^4} \frac{\mathrm{Tr}[(\not{q} + \not{k} + m)\gamma_\mu(\not{k} + m)\gamma_\nu]}{[(q+k)^2 - m^2][k^2 - m^2]}$$

  - Use **Feynman identity**:

$$\frac{1}{[(q+k)^2 - m^2][k^2 - m^2]} = \int_0^1 \mathrm{d}x \frac{1}{[k'^2 - \Delta_\gamma + \mathrm{i}\epsilon]^2}$$

$$k' = k + xq, \; \Delta_\gamma = -x(1-x)q^2 + m^2$$

Radiative Correction at $\mathcal{O}(e^4)$ in QED

- **(c) photon vacuum polarization**
  - Separate divergence powers:

$$\mathrm{i}\Pi^{[2]}_{\mu\nu}(\mathrm{q}^2) = -4e^2\int_0^1 \mathrm{d}x\left\{\int \frac{\mathrm{d}^4k'}{(2\pi)^4}\left[\frac{2k'_\mu k'_\nu}{(k'^2-\Delta_\gamma+\mathrm{i}\epsilon)^2} - \frac{g_{\mu\nu}}{(k'^2-\Delta_\gamma+\mathrm{i}\epsilon)}\right]\right\} \leftarrow \textbf{quadratic divergence?}$$

$$+8e^2(q_\mu q_\nu - g_{\mu\nu}q^2)\int_0^1 \mathrm{d}x\int\frac{\mathrm{d}^4k'}{(2\pi)^4}\frac{x(1-x)}{(k'^2-\Delta_\gamma+\mathrm{i}\epsilon)^2} \quad \leftarrow \textbf{logarithmic divergence}$$

  - Quadratic divergence cancels in dimensional regularization
  - Remaining (logarithmic divergent) term is **gauge invariant**:

$$q^\mu\Pi^{[2]}_{\mu\nu} = q^\nu\Pi^{[2]}_{\mu\nu} = 0$$

$$\mathrm{i}\Pi^{[2]}_{\mu\nu}(q^2) \equiv \mathrm{i}(q^2g_{\mu\nu} - q_\mu q_\nu)\Pi^{[2]}_\gamma(q^2)$$

  - **Renormalize:** EM gauge field strength & photon self-energy

$$Z_3^{[2]} = 1 + \Pi^{[2]}_\gamma(0)$$

$$\frac{-\mathrm{i}g_{\mu\nu}}{q^2} \to \frac{-\mathrm{i}g_{\mu\nu}}{q^2(1-\bar{\Pi}_\gamma(q^2))} \qquad \bar{\Pi}^{[2]}_\gamma(q^2) = \Pi^{[2]}_\gamma(q^2) - \Pi^{[2]}_\gamma(0)$$

  - Gauge invariance (requires $m_\gamma = 0$) is kept since pole is still at $q^2 = 0$

Radiative Correction at $\mathcal{O}(e^4)$ in QED

- **(c) physics of photon self-energy**

$$\bar{\Pi}_\gamma^{[2]}(q^2) = -\frac{2\alpha}{\pi}\int_0^1 dx\, x(1-x)\ln\left[\frac{m^2}{m^2 - q^2 x(1-x)}\right]$$

- **Modified Coulomb's law**

In the static limit $q_0 = 0$, and low-momentum (large distance) limit $\vec{q}^2 \ll m^2$:

$$\bar{\Pi}_\gamma^{[2]}(q^2) \approx +\frac{2\alpha}{\pi}\int_0^1 dx\, x^2(1-x)^2 \cdot \frac{\vec{q}^2}{m^2} = +\frac{\alpha}{15\pi}\frac{\vec{q}^2}{m^2}$$

The photon propagator is approximated by

$$\frac{-ig_{\mu\nu}}{q^2}\left[1 + \bar{\Pi}^{[2]}(q^2)\right] = ig_{\mu\nu}\left[\frac{1}{\vec{q}^2} + \frac{\alpha}{15\pi}\cdot\frac{1}{m^2}\right]$$

In Fourier transform:

$$\frac{1}{\vec{q}^2} \rightarrow \frac{1}{4\pi r}$$

$$1 \rightarrow \delta^3(\vec{r})$$

This leads to the Coulomb potential:

$$V(r) = -\left[\frac{\alpha}{r} + \frac{4\alpha^2}{15m^2}\delta^3(\vec{r})\right]$$

A short-range correction to Coulomb's law

- **Running Coupling / effective charge**

$$\alpha(q^2) = \alpha[1 + \bar{\Pi}_\gamma^{[2]}(q^2)] \qquad e^2(q^2) = e^2[1 + \bar{\Pi}_\gamma^{[2]}(q^2)]$$

- Interpret running e^2 as **screening effects**: at $r > m^{-1}$ ($|q^2| < m^2$), the virtual e^+e^- pair makes the vacuum a dielectric medium, where the "screened" charge is less than the "bare" charge

$$\boldsymbol{e = e_0/\epsilon(r)}$$

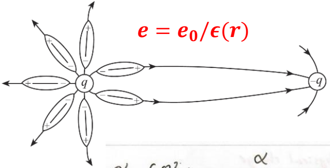

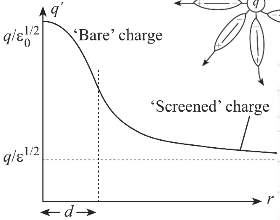

$$\alpha_{eff}(Q^2) = \frac{\alpha}{1 - \Delta\alpha(Q^2)};$$

$$\Delta\alpha(Q^2) = \frac{\alpha}{3\pi}\sum_l \ln\frac{Q^2}{Am_l}$$

for all $m_l^2 \ll Q^2$

Radiative Correction at $\mathcal{O}(e^4)$ in QED

- **(d) vertex correction**

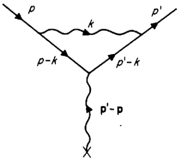

$$\Gamma_\mu^{[2]}(p, p') = -\mathrm{i}e^2 \int \frac{1}{k^2}\gamma^\lambda \frac{1}{\not{p}' - \not{k} - m}\gamma_\mu \frac{1}{\not{p} - \not{k} - m}\gamma_\lambda \frac{\mathrm{d}^4 k}{(2\pi)^4}$$

  - Logarithmic divergence is canceled by Z_1counter term
  - $Z_1$is charge renormalization constant

$$Z_1 e = e_0 Z_2 Z_3^{1/2}$$

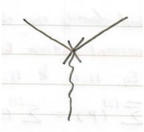

  - **Renormalization at q=0:**

$$\Gamma_\mu^{[2]}(p, p) + \gamma_\mu (Z_1^{[2]} - 1) = 0$$

  - **Ward Identity:**

$$-\frac{\partial \Sigma^{[2]}}{\partial p^\mu} = \Gamma_\mu^{[2]}(p, p' = p) \quad \Rightarrow Z_1 = Z_2; \quad e = e_0 Z_3^{1/2}$$

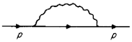

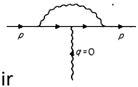

Charge universality: if two different fermions have the same bare charge e_0, their physical charge e are the same, and are independent of fermion masses.

Radiative Correction at $\mathcal{O}(e^4)$ in QED

- **(d) vertex correction**
  - Anomalous magnetic moment

$$\rightarrow -ie\bar{u}(p',s')\left[F_1(q^2) + i\kappa \frac{F_2(q^2)}{2m}\sigma_{\mu\nu} q^\nu\right] u(p,s)$$

fermion form factors (sec. 8.8)

magnetic moment g-factor:

$$g/2 = 1+\kappa$$

Contributions to F_1 & F_2

F_1 : $\bar{T}_\mu$ & $\bar{\Pi}_\gamma$

κF_2 : $\bar{T}_\mu$ only

In standard model physics

$\kappa_e = \frac{\alpha}{2\pi} \approx 0.0011614$ ⇐ electron

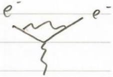

$\kappa_\mu \simeq 0.0011659$ ⇐ muon

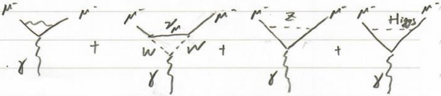

Lamb Shift & Radiative Correction Theory

- **In $e - p$ scattering, radiative correction only contributes to the mass and charge renormalization.**
- **In $e\mathrm{H}$ bound states, radiative correction produces observable level shift**
- **In Bethe's calculation:**
  - **Level shift is due to the difference between self-energies of bound and free electrons**
  - Interaction Hamiltonian is $H_I = -\frac{e}{m}\boldsymbol{A}(\boldsymbol{x}) \cdot \boldsymbol{p}$
  - Electron self-energy correction can be evaluated by 2nd order perturbation in electric dipole approximation

$$\delta E(nl) = -\sum_{\lambda}\sum_{r=1,2}\left(\frac{e}{m}\right)^2 \int \frac{d^3k}{(2\pi)^3} \frac{|\langle\lambda|\boldsymbol{\epsilon}_r(\boldsymbol{k})\cdot\boldsymbol{p}|nl\rangle|^2}{2k(E_\lambda + k - E_n)}$$

$$= -\frac{1}{6\pi^2}\left(\frac{e}{m}\right)^2 \sum_{\lambda} |\langle\lambda|\boldsymbol{p}|nl\rangle|^2 \int_0^\infty dk \frac{k}{E_\lambda + k - E_n}$$

← linear divergence at $k \to \infty$

  - $\epsilon_{1,2}$ are the photon polarization directions, $|\lambda\rangle$ consists the complete set of intermediate atomic states, and we used the fact

$$\sum_{r=1,2} |\langle\lambda|\boldsymbol{\epsilon}_r(\boldsymbol{k})\cdot\boldsymbol{p}|nl\rangle|^2 = \sin^2\theta\,|\langle\lambda|\boldsymbol{p}|nl\rangle|^2$$

Bethe, Phys. Rev. 72, 339 (1947)
Mandl, Shaw, Quantum Field Theory

Lamb Shift & Radiative Correction Theory

- **In Bethe's calculation:**
  - For a free electron, the self-energy correction can also be evaluated based on 2nd order perturbation between plane wave states, which provides the **mass renormalization**
  - The corresponding **mass correction** for the electron in the $|nl\rangle$ state is

$$\delta E_f(nl) == -\frac{1}{6\pi^2}\left(\frac{e}{m}\right)^2 \sum_\lambda |\langle\lambda|\boldsymbol{p}|nl\rangle|^2 \int_0^\infty dk$$

← linear divergence at $k \to \infty$

  - Since the physical electron mass is used in calculating $\delta E(nl)$, the mass correction is already included.
  - The **observed level shift $\Delta E(nl)$** is the difference between self-energies of bound and free electrons

$$\begin{aligned}\Delta E(nl) =& \delta E(nl) - \delta E_f(nl) \\ =& -\frac{1}{6\pi^2}\left(\frac{e}{m}\right)^2 \sum_\lambda |\langle\lambda|\boldsymbol{p}|nl\rangle|^2 \int_0^\infty dk \frac{E_\lambda - E_n}{E_\lambda + k - E_n}\end{aligned}$$

  - Introduce an ultraviolet hard momentum **cutoff** $K \sim m \gg |E_\lambda - E_n|$

$$\Delta E(nl) = \frac{1}{6\pi^2}\left(\frac{e}{m}\right)^2 \sum_\lambda |\langle\lambda|\boldsymbol{p}|nl\rangle|^2 (E_\lambda - E_n) \ln \frac{K}{|E_\lambda - E_n|}$$

Bethe, Phys. Rev. 72, 339 (1947)
Mandl, Shaw, Quantum Field Theory

Lamb Shift & Radiative Correction Theory

- **In Bethe's calculation:**
  - Summation over intermediate states:

$$\sum_\lambda |\langle\lambda|\boldsymbol{p}|nl\rangle|^2 (E_\lambda - E_n) = 2\pi\alpha|\phi_{nl}(0)|^2 = (2\alpha^4 m^3/n^3)\delta_{l0}$$

define a log-average excitation

$$\ln\langle E_\lambda - E_n\rangle = \frac{\sum_\lambda |\langle\lambda|\boldsymbol{p}|nl\rangle|^2 (E_\lambda - E_n)\ln|E_\lambda - E_n|}{\sum_\lambda |\langle\lambda|\boldsymbol{p}|nl\rangle|^2 (E_\lambda - E_n)}$$

$$\Delta E(nl) = \frac{8\alpha^3}{3\pi n^3}\mathrm{Ry}\ \ln\frac{K}{\langle E_\lambda - E_n\rangle},$$

$\mathrm{Ry} = m\alpha^2/2 = 13.6\,\mathrm{eV}$ **Rydberg energy**

  - Bethe took $K = m_e$ and $\langle E_\lambda - E_{2s}\rangle = 17.8$ Ry, and obtain

$$E(2s_{1/2}) - E(2p_{1/2}) = 1040\ \mathrm{MHz}$$

    - in remarkable agreement with experiment value 1057.8(1) MHz
    - Electron self-energy explains the bulk of Lamb shift in hydrogen

Beth, Phys. Rev. 72, 339 (1947)
Mandl, Shaw, Quantum Field Theory

Lamb Shift & Radiative Correction Theory

- **Photon vacuum polarization correction (Uehling Effect):**
  - Introduce a short-range modification to the Coulomb potential between ep

$$-\frac{\alpha}{r} \to -\frac{\alpha}{r} - \frac{4\alpha^2}{15\pi m_e^2}\delta^3(\boldsymbol{r})$$

  - The vacuum polarization makes a 1st order perturbative correction to atomic levels

$$\Delta E_{\rm vp}(nl) \quad = \quad \langle nl|V_{vp}|nl\rangle = -\frac{4\alpha^2}{15 m_e^2}|\phi_{nl}(0)|^2 = -\frac{8\alpha^3}{15\pi n^3}{\rm Ry}\,\delta_{l0}$$

  - Uehling effect's correction in hydrogen is subleading

$$E(2s_{1/2}) - E(2p_{1/2}) = -27 \text{ MHz}$$

- **Lamb Shift offers an important test ground for bound state QED**

Beth, Phys. Rev. 72, 339 (1947)
Mandl, Shaw, Quantum Field Theory

Lamb Shift in Muonic Hydrogen

- **Muon mass is ~210 times of electron mass**
- **Radiative Corrections in muonic hydrogen indicate a different hierarchy**
- **Lepton Self Energy:**

$$\Delta E(nl) = \frac{8\alpha^3}{3\pi n^3}\mathrm{Ry}\ \ln\frac{K}{\langle E_\lambda - E_n\rangle}\delta_{lo}$$

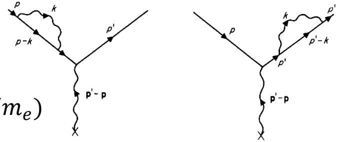

  - Ry, K & $\langle E_\lambda - E_n\rangle$ are enhanced by the factor (m_μ/m_e)
  - $\Delta E_{2s,se}(\mu H) \approx 210\ \Delta E_{2s,se}(eH) \approx 220\ \text{GHz}$
- **Vacuum Polarization:**

$$\Delta E_{\rm vp}(nl) = -\frac{4\alpha^2}{15m_e^2}|\phi_{nl}(0)|^2$$

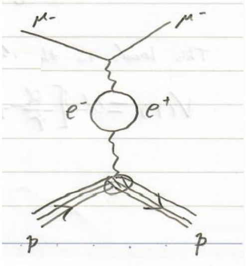

  - $|\phi_{nl}(0)|^2$ is enhanced by $(m_\mu/m_e)^3$
  - $\Delta E_{2s,vp}(\mu H) \approx (210)^3\ \Delta E_{2s,vp}(eH) \approx -250\ \text{THz}$
- **Vacuum polarization (Uehling effect) dominates in Lamb shift in muonic hydrogen**

Nuclear electric radius from Lamb shift

- Extract the nuclear electric radius R_E from Lamb shift in light muonic atoms

$$\delta E_{\rm LS} = \delta_{\rm QED} + \mathcal{A}_{\rm OPE}\, R_E^2 + \delta_{\rm TPE}$$

Nuclear electric radius from Lamb shift

- Extract the nuclear electric radius R_E from Lamb shift in light muonic atoms

$$\delta E_{\rm LS} = \delta_{\rm QED} + \mathcal{A}_{\rm OPE}\, R_E^2 + \delta_{\rm TPE}$$

- **QED corrections:**
  - vacuum polarization
  - lepton self energy
  - relativistic recoil effects

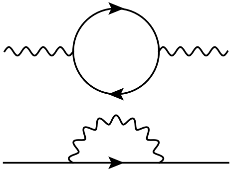

Nuclear electric radius from Lamb shift

- Extract the nuclear electric radius R_E from Lamb shift in light muonic atoms

$$\delta E_{\rm LS} = \delta_{\rm QED} + \mathcal{A}_{\rm OPE}\, R_E^2 + \delta_{\rm TPE}$$

- **Nuclear structure effects:**

Nuclear electric radius from Lamb shift

- Extract the nuclear electric radius R_E from Lamb shift in light muonic atoms

  $$\delta E_{\rm LS} = \delta_{\rm QED} + \boxed{\mathcal{A}_{\rm OPE}\, R_E^2} + \delta_{\rm TPE}$$

- **Nuclear structure effects:**
  - **linear to $R_E^2 \Longrightarrow$ structure effects in one photon exchange**
    $\mathcal{A}_{\rm OPE} \approx m_\mu^3 (Z\alpha)^4/12$

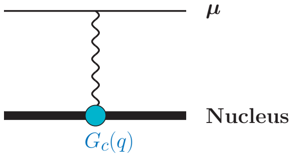

Nuclear electric radius from Lamb shift

- Extract the nuclear electric radius R_E from Lamb shift in light muonic atoms

$$\delta E_{\rm LS} = \delta_{\rm QED} + \boxed{\mathcal{A}_{\rm OPE}\, R_E^2} + \delta_{\rm TPE}$$

- **Nuclear structure effects:**
  - **linear to $R_E^2 \Longrightarrow$ structure effects in one photon exchange**
    $\mathcal{A}_{\rm OPE} \approx m_\mu^3 (Z\alpha)^4/12$

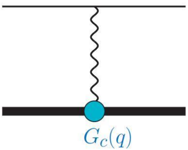

- $G_c(q^2) \approx 1 - \frac{1}{6} R_E^2\, q^2 + \cdots$
- Modification to Coulomb interaction:
- $\frac{1}{q^2} \to \frac{1}{q^2}\left(1 - \frac{1}{6} R_E^2\, q^2\right)$
- Fourier transform: $-\frac{Z\alpha}{r} \to -\frac{Z\alpha}{r} - \frac{2\pi}{3} Z\alpha R_E^2 \delta^3(\boldsymbol{r})$
- Similar to VP correction, the 1st order perturbation leads to:

$$\mathcal{A}_{\rm OPE} \approx \frac{2\pi}{3} Z\alpha |\phi_{nl}(0)|^2$$

Nuclear electric radius from Lamb shift

- Extract the nuclear electric radius R_E from Lamb shift in light muonic atoms

$$\delta E_{\mathrm{LS}} = \delta_{\mathrm{QED}} + \mathcal{A}_{\mathrm{OPE}}\, R_E^2 + \boxed{\delta_{\mathrm{TPE}}}$$

- **Nuclear structure effects:**
  - $\boldsymbol{\delta_{\mathrm{TPE}}} \Longrightarrow$ **structure effects in two photon exchange** $(Z\alpha)^5$
  - elastic: Zemach contribution δ_{Zem}
    $\delta_{\mathrm{Zem}} \propto \iint d\boldsymbol{r} d\boldsymbol{r}' \rho_E(\boldsymbol{r})\, \rho_E(\boldsymbol{r}')\, |\boldsymbol{r} - \boldsymbol{r}'|^3$
  - inelastic: polarizability effect δ_{pol}

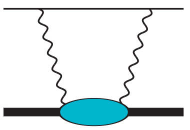

Nuclear electric radius from Lamb shift

- Extract the nuclear electric radius R_E from Lamb shift in light muonic atoms

$$\delta E_{\rm LS} = \delta_{\rm QED} + \mathcal{A}_{\rm OPE}\, R_E^2 + \boxed{\delta_{\rm TPE}}$$

- **Nuclear structure effects:**
  - $\boldsymbol{\delta_{\rm TPE}} \Longrightarrow$ **structure effects in two photon exchange** $(Z\alpha)^5$
  - elastic: Zemach contribution $\delta_{\rm Zem}$
    $\delta_{\rm Zem} \propto \iint d\boldsymbol{r} d\boldsymbol{r}' \rho_E(\boldsymbol{r})\, \rho_E(\boldsymbol{r}')\, |\boldsymbol{r} - \boldsymbol{r}'|^3$
  - inelastic: polarizability effect $\delta_{\rm pol}$

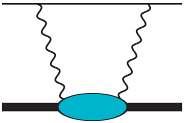

- **Accuracy in extracting R_E relies on $\delta_{\rm TPE}$ input**
  e.g., μ^2H: $\delta_{\rm pol}$ requires a 1% accuracy
  $\mu^{3,4}$He$^+$: $\delta_{\rm pol}$ requires a 5% accuracy

Hadronic & nuclear two-photon exchange

- The separation of hadronic/nuclear scales ($\Lambda_\chi \gg m_\pi$) allows the separation of hadronic/nuclear parts of $\delta_{\rm TPE}$

$$\delta_{\rm TPE} = \delta^N_{\rm TPE} + \delta^A_{\rm TPE}$$

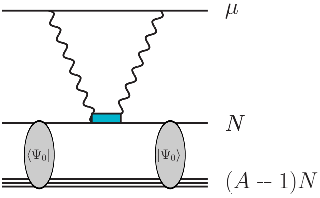

$$\delta^N_{\rm TPE} = \delta^N_{\rm Zem} + \delta^N_{\rm pol}$$

dispersion analysis
Carlson, Vanderhaeghen, PRA 2011
Birse, McGovern, EPJA 2012

Hadronic & nuclear two-photon exchange

- The separation of hadronic/nuclear scales ($\Lambda_\chi \gg m_\pi$) allows the separation of hadronic/nuclear parts of $\delta_{\rm TPE}$

$$\delta_{\rm TPE} = \delta^N_{\rm TPE} + \delta^A_{\rm TPE}$$

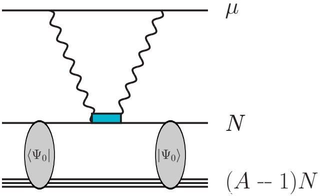

$$\delta^N_{\rm TPE} = \delta^N_{\rm Zem} + \delta^N_{\rm pol}$$

dispersion analysis
Carlson, Vanderhaeghen, PRA 2011
Birse, McGovern, EPJA 2012

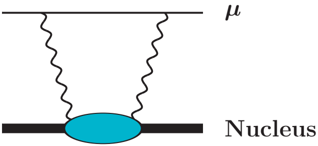

$$\delta^A_{\rm TPE} = \delta^A_{\rm Zem} + \delta^A_{\rm pol}$$

dispersion analysis
photo-disintegration data
ab initio calculation

Two-photon exchange diagrams

- Evaluate δ_{pol} from the two-photon exchange diagrams

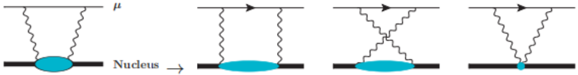

- Level shift: $$\Delta E_{nl} = -\frac{(4\pi\alpha)^2}{m}|\varphi_{nl}(0)|^2 \,\mathrm{Im}\int \frac{d^4q}{(2\pi)^4} D^{\mu\rho}(q) D^{\nu\tau}(-q) t_{\mu\nu}(q,k) T_{\rho\tau}(q,-q)$$

- Nuclear forward virtual Compton amplitude

$$T_{\rho\tau}(q,-q) = \text{seagull} + \sum_{n\neq 0}\left\{\frac{\langle 0|\hat{J}_\rho(0)|nq\rangle\langle nq|\hat{J}_\tau(0)|0\rangle}{E_0-E_n+q_0+i\varepsilon} + \frac{\langle 0|\hat{J}_\tau(0)|n-q\rangle\langle n-q|\hat{J}_\rho(0)|0\rangle}{E_0-E_n-q_0+i\varepsilon}\right\}$$

- Lepton tensor

$$it^{\mu\nu}(q,k) = \bar{u}(k)(-i\gamma^\mu)\, i\frac{\not k - \not q + m}{(k-q)^2 - m^2 + i\epsilon}(-i\gamma^\nu)u(k)$$

$$= -i\,\bar{u}(k)\gamma^\mu \frac{\not k - \not q + m}{(k-q)^2 - m^2 + i\epsilon}\gamma^\nu u(k)$$

$$t^{\mu\nu}(q,k) = -\frac{1}{2}\sum_s \bar{u}^s_a(k)\gamma^\mu_{ab}\frac{(\not k - \not q + m)_{bc}}{(k-q)^2 - m^2 + i\epsilon}\gamma^\nu_{cd}u^s_d(k)$$

$$= -\frac{1}{2}\gamma^\mu_{ab}\frac{(\not k - \not q + m)_{bc}}{(k-q)^2 - m^2 + i\epsilon}\gamma^\nu_{cd}\left[\sum_s u^s(k)\bar{u}^s(k)\right]_{da}$$

$$= -\frac{1}{2}\cdot\frac{tr[\gamma^\mu(\not k - \not q + m)\gamma^\nu(\not k + m)]}{(k-q)^2 - m^2 + i\epsilon}$$

$$= -\frac{1}{2}\cdot\frac{k\cdot q\, g^{\mu\nu} + (k-q)^\mu k^\nu + k^\mu (k-q)^\nu}{(k-q)^2 - m^2 + i\epsilon}$$

- In Lamb shift, take spin average

$$\frac{1}{2}\sum_s u^s(p)\bar{u}^s(p) = \not p + m$$

Rosenfelder, Nucl. Phys. A, 393, 301 (1983)

Two-photon exchange diagrams

- With **crossing symmetry**, TPE corrections to the Lamb shift is separated into a longitudinal and transverse polarization part

$$\Delta E_{nl} = (4\pi\alpha)^2 |\varphi_{nl}(0)|^2 \,\mathrm{Im} \int \frac{\mathrm{d}^4 q}{(2\pi)^4} \frac{2m}{(q^2+i\varepsilon)^2 - 4m^2 q_0^2} \left\{ \frac{1}{\boldsymbol{q}^2} T_{\mathrm{L}} + \frac{q_0^2}{(q^2+i\varepsilon)^2} T_{\mathrm{T}} \right\}$$

  - Forward virtual Compton amplitudes

$$T_{\mathrm{L}} = T_{00}, \qquad T_{\mathrm{L}}(q_0, \boldsymbol{q}) = \int_0^\infty \mathrm{d}\omega\, S_{\mathrm{L}}(\omega, \boldsymbol{q}) \left\{ \frac{1}{q_0 - \omega + i\varepsilon} - \frac{1}{q_0 + \omega - i\varepsilon} \right\},$$

$$T_{\mathrm{T}} = \left(\delta_{ij} - \frac{q_i q_j}{\boldsymbol{q}^2} \right) T^{ij} \qquad T_{\mathrm{T}}(q_0, \boldsymbol{q}) = \text{seagull} + \int_0^\infty \mathrm{d}\omega\, S_{\mathrm{T}}(\omega, \boldsymbol{q}) \left\{ \frac{1}{q_0 - \omega + i\varepsilon} - \frac{1}{q_0 + \omega - i\varepsilon} \right\}$$

  - Nuclear polarization response function

$$S_{\mathrm{L,T}}(\omega, \boldsymbol{q}) = \sum_{n \neq 0} \delta(\omega - (E_n - E_0)) |\langle n | \mathcal{O}_{\mathrm{L,T}}(\boldsymbol{q}) | 0 \rangle|^2$$

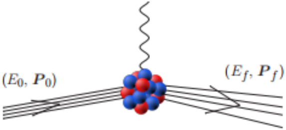

  - Integrate over q_0:

$$\Delta E_{nl} = -8\alpha^2 |\varphi_{nl}(0)|^2 \int_0^\infty \mathrm{d}|\boldsymbol{q}| [R_{\mathrm{L}} + R_{\mathrm{T}} + R_{\mathrm{S}}]$$

$$R_{L,T,S} = \int d\omega\, g_{L,T,S}(\omega, q) S_{L,T,S}(\omega, q)$$

R_S: seagull term

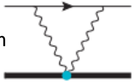

Rosenfelder, Nucl. Phys. A, 393, 301 (1983)

Nuclear polarizability in NR quantum mechanics

- Hamiltonian for muonic atoms

$$H = H_{nucl} + H_\mu + \Delta H$$

$$H_\mu = \frac{p^2}{2m_r} - \frac{Z\alpha}{r}$$

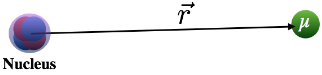

Nuclear polarizability in NR quantum mechanics

- Hamiltonian for muonic atoms

$$H = H_{nucl} + H_\mu + \Delta H$$

$$H_\mu = \frac{p^2}{2m_r} - \frac{Z\alpha}{r}$$

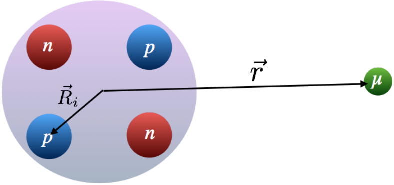

- Corrections to the point Coulomb

$$\Delta H = \alpha \sum_i^Z \Delta V(\boldsymbol{r}, \boldsymbol{R}_i) \equiv \alpha \sum_i^Z \left(\frac{1}{r} - \frac{1}{|\boldsymbol{r} - \boldsymbol{R}_i|} \right)$$

- δ^A_{pol}: ΔH's 2^{nd}-order perturbative effects to the atomic spectrum
  - inelastic part of 2γ exchange
  - nucleus excited in intermediate states

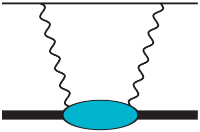

Evaluate $\delta_{\rm pol}$ by nuclear sum rules

$$\delta_{\rm pol} = \sum_{g, S_{\hat{O}}} \int_{\omega_{th}}^{\infty} d\omega \underbrace{g(\omega)}_{\text{weight func}} \underbrace{S_{\hat{O}}(\omega)}_{\text{response func}}$$

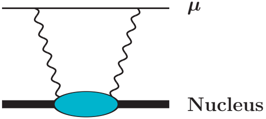

- energy-dependent weight $g(\omega)$
- nuclear response function $S_{\hat{O}}(\omega)$

$$S_O(\omega) = \sum\!\!\!\!\!\!\int_f |\langle\psi_f|\hat{O}|\psi_0\rangle|^2 \delta(E_f - E_0 - \omega)$$

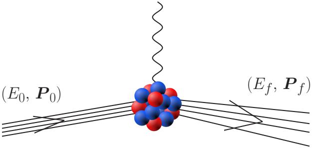

Evaluate δ_{pol} by nuclear sum rules

$$\delta_{\text{pol}} = \sum_{g, S_{\hat{O}}} \int_{\omega_{th}}^{\infty} d\omega \, \underbrace{g(\omega)}_{\text{weight func}} \, \underbrace{S_{\hat{O}}(\omega)}_{\text{response func}}$$

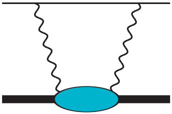

Contributions to δ_{pol} in muonic atoms

- multipolarity expansion of electromagnetic operator
  - sum rules of E0, E1, E2, M1 responses
- muon relativistic and Coulomb-distortion corrections
- intrinsic nucleon charge-distribution corrections

CJ, Bacca, Barnea, Hernandez, Nevo-Dinur, JPG 45 (2018) 093002

Determination of $\delta^A_{\rm pol}$

- extract $S_{\hat{O}}(\omega)$ from photoabsorption data
  - μ^3He$^+$: Rinker '76 20% uncertainty
  - μ^4He$^+$: Bernabeu & Jarlskog '74; Rinker '76; Friar '77 20% uncertainty
- from scattering data (dispersion analysis)
  - $\mu\,^2$H: Carlson, Gorchtein, Vanderhagen '14 35% uncertainty
  - $\mu\,^3$He$^+$: Carlson, Gorchtein, Vanderhaeghen '17 3% uncertainty
- To improve accuracy → ab initio calculations

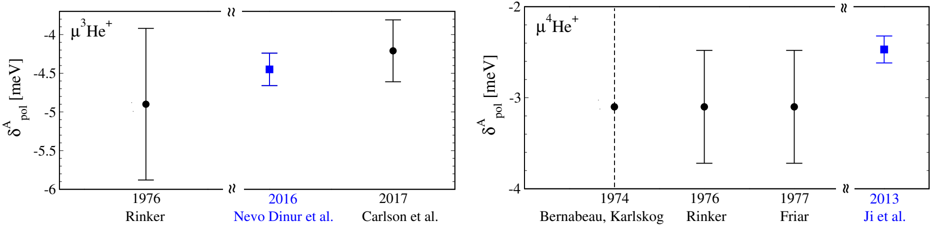

$\delta_{\rm pol}^{A}$ in electronic atoms

- In ^{6,8}He and ^{11}Li spectroscopy, $\delta_{\rm pol}^{A}$ was determined by photo-absorption data
- The shallow binding (halo structure) in ^{6,8}He and ^{11}Li makes $\delta_{\rm pol}^{A}$ non-negligible
- high-precision photo-absorption data is not required in electronic atoms
- photo-absorption data:

^{6}He

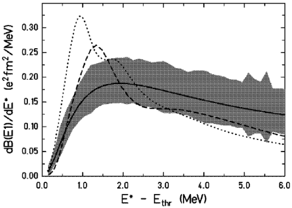

^{8}He

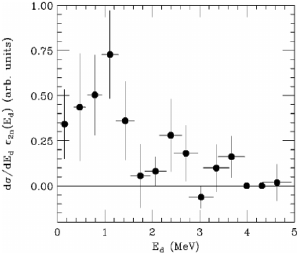

^{11}Li

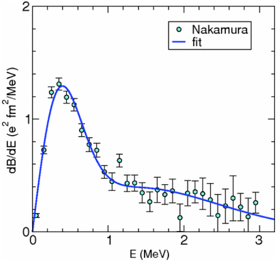

Determine $S_{\hat{O}}$ from photo-disintegration data

$\sigma_\gamma(\omega) = 4\pi^2 \alpha \omega S_{E1}(\omega)$

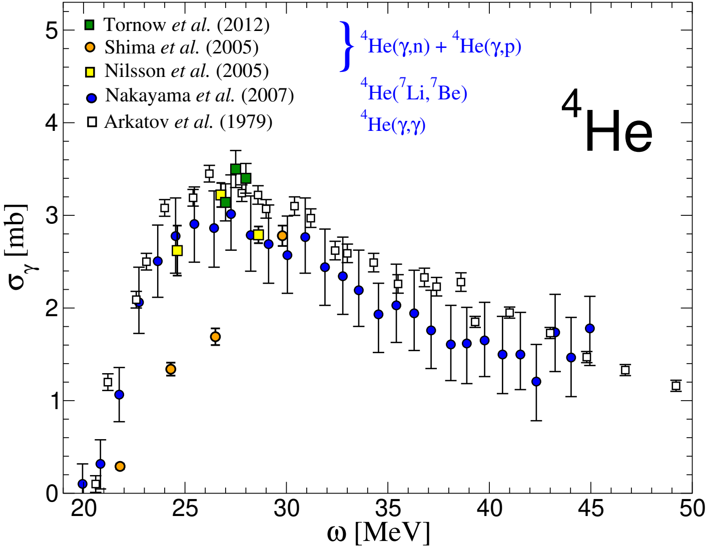

Determine $S_{\hat{O}}$ from photo-disintegration data

$$\sigma_\gamma(\omega) = 4\pi^2\alpha\omega S_{E1}(\omega)$$

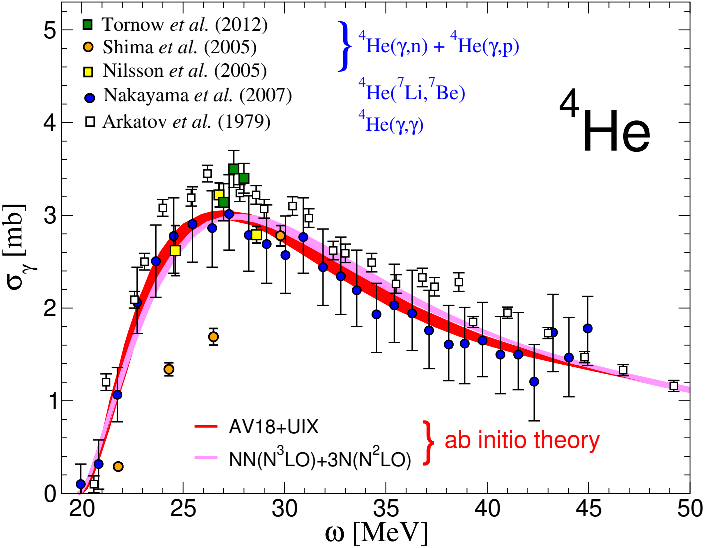

Determine $\delta_{\rm pol}$ from ab initio theory

- $\mu^{2,3}$H, $\mu^{3,4}$He$^+$:
  - Few-body methods
    - solve nuclear few-body Schrödinger equations in nucleon degrees of freedom
    - deal with both bound-state and continuum problems
  - Nuclear Hamiltonian Models
    - use modern two-nucleon & three-nucleon potentials
      AV18+UIX
      χEFT NN(N^{3}LO)+NNN(N^{2}LO)
      pionless EFT

pionless effective field thoery

- $\not{\pi}$EFT describes ^{2}H and np (^{3}S$_1$) scattering with contact interactions only
- low-momentum prediction depends on only a_t, r_t at NNLO (3% accuracy)

$$\mathcal{L} = N^\dagger \left[i\partial_0 + \frac{\nabla^2}{2M} \right] N - C_0 \left(N^T P_i N\right)^\dagger \left(N^T P_i N\right)$$
$$+ \frac{C_2}{8} \left[\left(N^T P_i N\right)^\dagger \left(N^T \overleftrightarrow{\partial}^2 P_i N\right) + h.c. \right] - \frac{C_4}{16} \left(N^T \overleftrightarrow{\partial}^2 P_i N\right)^\dagger \left(N^T \overleftrightarrow{\partial}^2 P_i N\right)$$

Kaplan, Savage, Wise, Nuclear Physics B 534 (1998) 329

- Order-by-order evaluation of scattering t-matrices $\mathcal{A}_n$

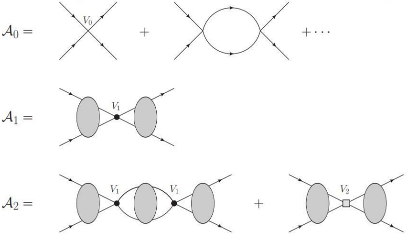

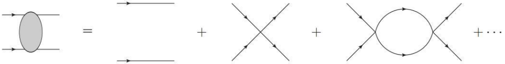

Order-by-order expansion of LECs

$$C_0 = C_{0,-1} + C_{0,0} + C_{0,1},$$
$$C_2 = C_{2,-2} + C_{2,-1},$$
$$C_4 = C_{4,-3},$$

Pionless effective field theory

- Solve n-p scattering in Lippmann Schwinger equations
  - Leading order

$$i\mathcal{A}_{\mathrm{LO}}(E) = -iC_{0,-1}\left[1 - \mathcal{I}_0(E)\mathcal{A}_{\mathrm{LO}}(E)\right]$$

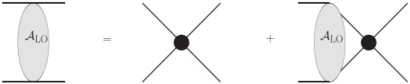

  - Next-to-leading order

$$i\mathcal{A}_{\mathrm{NLO}}(k,p;E) = -iC_{0,0}[1 + i\mathcal{I}_0 i\mathcal{A}_{\mathrm{LO}}]^2 - iC_{2,-2}(1 + i\mathcal{I}_0 i\mathcal{A}_{\mathrm{LO}})\left[\frac{k^2+p^2}{2} + i\mathcal{I}_2 i\mathcal{A}_{\mathrm{LO}}\right]$$

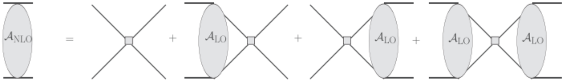

  - Loop integral in DR & power-divergence-subtraction scheme

$$\mathcal{I}_{2n}^{\mathrm{PDS}}(E) = i\int \frac{\mathrm{d}^4 q}{(2\pi)^4} q^{2n} S(q_0+E,\boldsymbol{q})S(-q_0,-\boldsymbol{q}) = -\frac{m_{\mathrm{N}}}{4\pi}p^{2n}(\mu + ip)$$

  - LECs from *np* phase shift

$$k\cot\delta_t = -\gamma + \frac{\rho_{\mathrm{d}}}{2}(k^2+\gamma^2) + \cdots$$

$$C_{0,-1} = -\frac{4\pi}{m_{\mathrm{N}}}\frac{1}{(\mu-\gamma)}, \qquad C_{2,-2} = \frac{2\pi}{m_{\mathrm{N}}}\frac{\rho_{\mathrm{d}}}{(\mu-\gamma)^2},$$

$$C_{0,0} = \frac{2\pi}{m_{\mathrm{N}}}\frac{\rho_{\mathrm{d}}\gamma^2}{(\mu-\gamma)^2}, \qquad C_{2,-1} = -\frac{2\pi}{m_{\mathrm{N}}}\frac{\rho_{\mathrm{d}}^2\gamma^2}{(\mu-\gamma)^3},$$

$$C_{0,1} = -\frac{\pi}{m_{\mathrm{N}}}\frac{\rho_{\mathrm{d}}^2\gamma^4}{(\mu-\gamma)^3}, \qquad C_{4,-3} = -\frac{\pi}{m_{\mathrm{N}}}\frac{\rho_{\mathrm{d}}^2}{(\mu-\gamma)^3},$$

Nuclear polarizability of μD in pionless EFT

- The nuclear polarizability effect is dominated by the **longitudinal polarization**
- Calculate the longitudinal **transition matrix elements** in pionless EFT
  - **Leading order**

$$\tilde{M}^{a}_{\mathrm{LO}} = -2m_{\mathrm{N}} / \left[\gamma^2 + (\boldsymbol{p} - \boldsymbol{q}/2)^2\right]$$
$$\tilde{M}^{b}_{\mathrm{LO}} = -2m_{\mathrm{N}} / \left[\gamma^2 + (\boldsymbol{p} + \boldsymbol{q}/2)^2\right]$$
$$\tilde{M}^{c}_{\mathrm{LO}} = 2\mathcal{J}_0 \mathcal{A}_{\mathrm{LO}}(E)$$

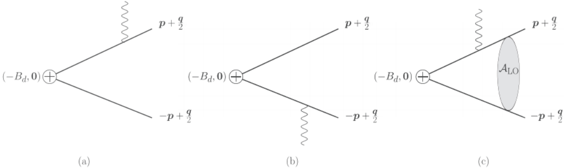

three-point loop
$$\mathcal{J}_{2n} = \int \frac{d^4 l}{(2\pi)^4} l^{2n} iS(-B_{\mathrm{d}} + l_0, \boldsymbol{l}) iS(-B_{\mathrm{d}} + l_0 + \omega, \boldsymbol{l} + \mathbf{q}) iS(-l_0, \boldsymbol{l})$$

  - **Next-to-leading order**

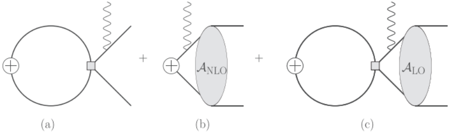

  - **Next-to-next-to-leading order**

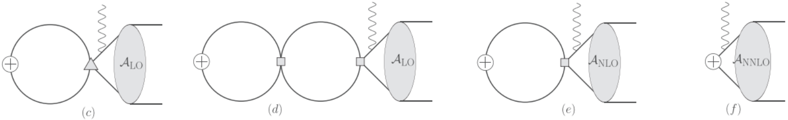

Nuclear polarizability of μD in pionless EFT

- Calculate nuclear **longitudinal polarization response function**
  - It is related to the transition matrix element by

$$S_L(\omega, \boldsymbol{q}) = \int \frac{d^3 p}{(2\pi)^3} \delta\left(\omega - B_d - \frac{q^2}{4m_N} - \frac{p^2}{m_N}\right) \overline{|\mathcal{M}|^2}$$

  - After spin average

$$\overline{|\mathcal{M}|^2} = \frac{\mathcal{Z}_d}{4}\left(\left|\frac{\tilde{M}^a - \tilde{M}^b}{2}\right|^2 + \left|\frac{\tilde{M}^a + \tilde{M}^b}{2} + \tilde{M}^c\right|^2\right)$$

  - Deuteron longitudinal response function

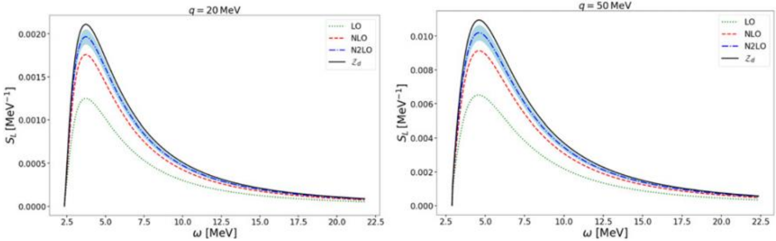

- order-by-order convergence of $S_L(\omega, q)$
- we can achieve 3% accuracy with only two input parameters (γ, ρ_d)

Emmons, CJ*, Platter, J. Phys. G 48, 035101 (2021)

Hypherspherical harmonic basis (few-body methods)

For heavier nucleus, one needs to go beyond the Lippmann-Schwinger equation and adopt a more powerful few-body methods to deal with bound-state and continuum-state few-body systems.

- Solve in the 3-body CM frame

  $[T+V]\psi(\vec{\eta}_1,\vec{\eta}_2) = E\psi(\vec{\eta}_1,\vec{\eta}_2)$

- Use hyperspherical coordinates

  $\rho = \sqrt{\eta_1^2+\eta_2^2}$, $\Omega = [\theta_1, \phi_1, \theta_2, \phi_2, \arctan(\frac{\eta_2}{\eta_1})]$

  $T = T_\rho + \hat{K}^2/\rho^2$

- hyperspherical harmonic basis expansion

$$\psi(\vec{\eta}_1,\vec{\eta}_2) \sim \sum_{[K]}^{K_{max}} R_{[K]}(\rho)\, \mathcal{Y}_{[K]}(\Omega)$$

$$\hat{K}^2\mathcal{Y}_{[K]}(\Omega) = K(K+4)\mathcal{Y}_{[K]}(\Omega)$$

3-body problem

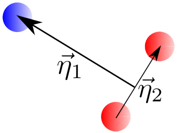

Hypersperical harmonics basis expansion

$$|\psi\rangle = \sum_{K}^{K_{max}} c_K \, \mathrm{HH}(K)$$

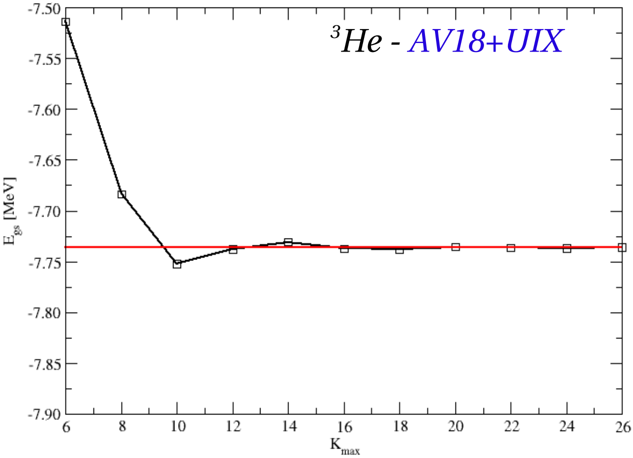

Response function: a continuum problem

- Nucleus is excited between two photons

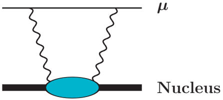

$$S_O(\omega) = \sum_f |\langle \psi_f | \hat{O} | \psi_0 \rangle|^2 \delta(E_f - E_0 - \omega)$$

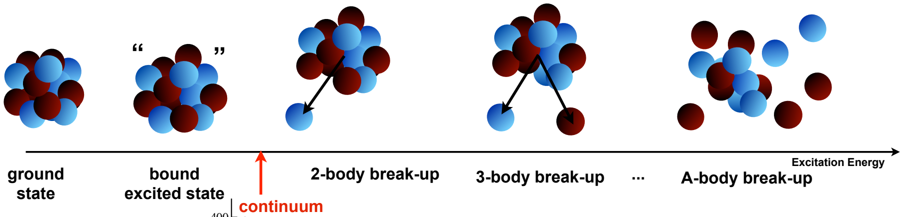

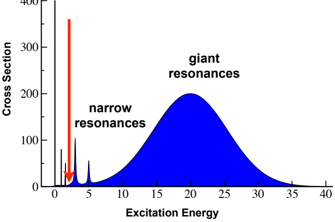

$$\sigma \propto |\langle \Psi_f | J^\mu | \Psi_0 \rangle|^2$$

Exact knowledge limited in energy and mass number

Lanczos algorithm for sum rules

- $\delta_{\rm pol} \Longrightarrow$ energy-dependent nuclear sum rules

$$I_{\hat{O}} = \int_0^\infty d\omega\, S_{\hat{O}}\left(\omega\right) g\left(\omega\right)$$

- Lanczos method can directly calculate I_O without explicitly knowing $S_{\hat{O}}\left(\omega\right)$.

- Map Hamiltonian in recursive Krylov subspace

$$\{\phi_0, \phi_1, \cdots, \phi_M\}$$

$$b_{i+1}|\phi_{i+1}\rangle = \hat{H}|\phi_i\rangle - a_i|\phi_i\rangle - b_i|\phi_{i-1}\rangle$$

$$|\phi_{-1}\rangle = 0; \quad |\phi_0\rangle = \hat{O}|\Psi_0\rangle; \quad \langle\phi_i|\phi_j\rangle = \delta_{ij}$$

- $I_{\hat{O}}$ converges when increasing Lanczos steps

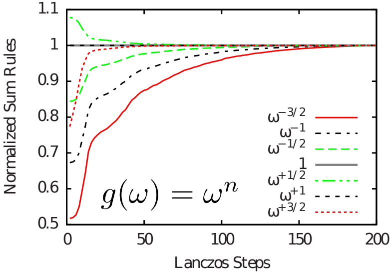

Nevo-Dinur, Barnea, CJ, Bacca, PRC **89**, 064317 (2014)

Two-photon exchange contributions

$\delta^A_{\rm TPE}$ in $\mu\,^3$He$^+$

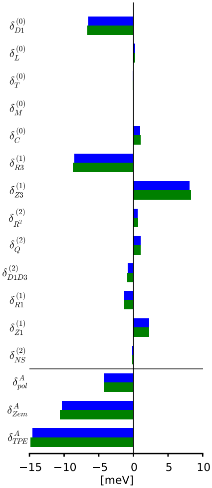

	AV18/UIX	χEFT
$\delta^{(0)}_{D1}$	-6.479	-6.633
$\delta^{(0)}_{L}$	0.232	0.240
$\delta^{(0)}_{T}$	-0.103	-0.107
$\delta^{(0)}_{M}$	0.006	0.006
$\delta^{(0)}_{C}$	1.000	1.020
$\delta^{(1)}_{R3}$	-8.539	-8.711
$\delta^{(1)}_{Z3}$	8.100	8.327
$\delta^{(2)}_{R^2}$	0.632	0.654
$\delta^{(2)}_{Q}$	1.015	1.038
$\delta^{(2)}_{D1D3}$	-0.841	-0.862
$\delta^{(1)}_{R1}$	-1.294	-1.314
$\delta^{(1)}_{Z1}$	2.256	2.291
$\delta^{(2)}_{NS}$	-0.193	-0.199
δ^{A}_{pol}	-4.208	-4.250
δ^{A}_{Zem}	-10.356	-10.618
δ^{A}_{TPE}	-14.564	-14.868

$\delta^A_{\rm TPE} = -14.72$ meV $\pm 1.5\% (1\sigma)$

$\delta_{\rm TPE}$ in $\mu\,^4$He$^+$

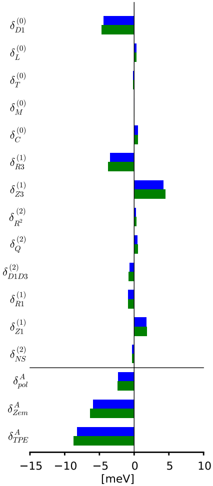

	AV18/UIX	χEFT
$\delta^{(0)}_{D1}$	-4.418	-4.701
$\delta^{(0)}_{L}$	0.289	0.308
$\delta^{(0)}_{T}$	-0.126	-0.134
$\delta^{(0)}_{M}$	0.008	0.006
$\delta^{(0)}_{C}$	0.519	0.553
$\delta^{(1)}_{R3}$	-3.442	-3.717
$\delta^{(1)}_{Z3}$	4.183	4.526
$\delta^{(2)}_{R^2}$	0.259	0.324
$\delta^{(2)}_{Q}$	0.484	0.561
$\delta^{(2)}_{D1D3}$	-0.666	-0.784
$\delta^{(1)}_{R1}$	-0.848	-0.874
$\delta^{(1)}_{Z1}$	1.753	1.811
$\delta^{(2)}_{NS}$	-0.279	-0.293
δ^{A}_{pol}	-2.284	-2.414
δ^{A}_{Zem}	-5.936	-6.337
δ^{A}_{TPE}	-8.220	-8.751

$\delta^A_{\rm TPE} = -8.49$ meV $\pm 4.4\% (1\sigma)$

Other uncertainties

Numerical uncertainty

- HH model space convergence ($\mu^4\mathrm{He}^+$)

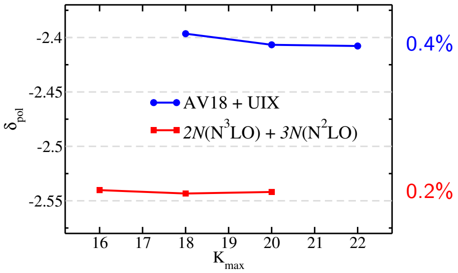

Atomic physics uncertainty

- $(Z\alpha)^6$ effects beyond 2^{nd} order perturbation
- relativistic & Coulomb corrections to multipoles other than dipole
- higher-order nucleon-size corrections
- The combination gives an additional uncertainty
  - 1.5% in $\mu^3\mathrm{He}^+$
  - 1.3% in $\mu^4\mathrm{He}^+$

- We combine all uncertainties in a quadratic sum
  $\delta^A_{\mathrm{TPE}}(\mu^3\mathrm{He}^+) = -14.72$ meV $\pm 2.1\%$
  $\delta^A_{\mathrm{TPE}}(\mu^4\mathrm{He}^+) = -8.49$ meV $\pm 4.6\%$
- comparable to 5% accuracy required in $\mu^{3,4}\mathrm{He}^+$ experiment

δ_{TPE} in light muonic atoms

$\delta_{\mathrm{TPE}} = [\delta^A_{\mathrm{Zem}} + \delta^A_{\mathrm{pol}}] + [\delta^N_{\mathrm{Zem}} + \delta^N_{\mathrm{pol}}]$

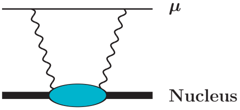

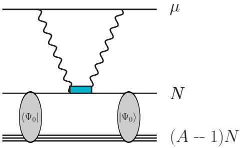

	δ^A_{Zem} (meV)	δ^A_{pol} (meV)	δ^N_{Zem} (meV)	δ^N_{pol} (meV)	δ_{TPE} (meV) [GHz]
μ^2H	−0.423(04)	−1.245(13)	−0.030(02)	−0.020(10)	−1.718(17) [415]
μ^3H	−0.227(06)	−0.480(11)	−0.033(02)	−0.031(17)	−0.771(22) [186]
μ^3He$^+$	−10.49(23)	−4.23(18)	−0.52(03)	−0.25(13)	−15.49(33) [3750]
μ^4He$^+$	−6.14(31)	−2.35(13)	−0.54(03)	−0.34(20)	−9.37(44) [2270]

μ^2H: Hernandez, CJ, Bacca, Nevo-Dinur, Barnea, PLB 736 (2014) 344
μ^3He$^+$ & μ^3H: Nevo Dinur, CJ, Bacca, Barnea, PLB 755 (2016) 380
μ^4He$^+$: CJ, Nevo-Dinur, Bacca, Barnea, PRL 111 (2013) 143402
review & update: CJ, Bacca, Barnea, Hernandez, Nevo-Dinur, JPG 45 (2018) 093002

charge radius from $\mu^2\mathrm{H}$ Lamb shift

- $r_d(\mu^2\mathrm{H})$ uncertainty is dominated by δ_{TPE} uncertainty

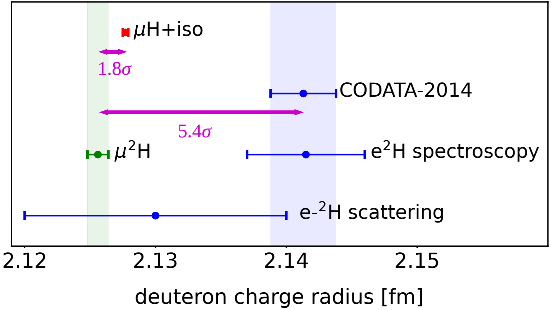

Pohl, *et al.*, Science 353, 669 (2016)

- δ_{TPE} inputs cited by Science 2016:
  - AV18: Pachucki, PRL 106 (2011) 193007; Pachucki, Wienczek, PRA 91 (2015) 040503
  - zero-range model: Friar, PRC 88 (2013) 034003
  - dispersion: Carlson, Gorchtein, Vanderhaeghen, PRA 89 (2014) 022504
  - AV18+χEFT: Hernandez, CJ*, Bacca, Nevo-Dinur, Barnea, PLB 736 (2014) 344

charge radius from $\mu^4\mathrm{He}^+$ Lamb shift

- $\mu^4\mathrm{He}^+$: $r_\alpha = 1.67824(13)_{\mathrm{exp}}(82)_{\mathrm{theo}}$
- r_E uncertainty is dominated by δ_{TPE} uncertainty

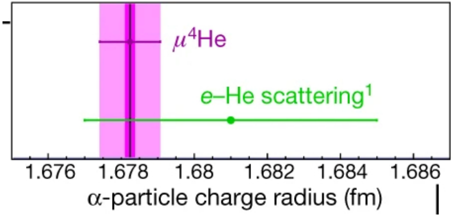

Krauth et al., Nature, 589, 527 (2021)

- δ_{TPE} inputs cited by Nature 2021:
  - Zemach moments:
    Sick, PRC 90 (2014) 064002
    Nevo-Dinur, Hernandez, Bacca, Barnea, CJ, Pastore, Piarulli, Wiringa, PRC 99 (2019) 034004
  - polarizability:
    CJ, Nevo-Dinur, Bacca, Barnea, PRL 111 (2013) 143402; FBS 55 (2014) 917
    CJ, Bacca, Barnea, Hernandez, Nevo-Dinur, JPG 45 (2018) 093002

Improve nuclear uncertainties

- further improvement in δ_{TPE} accuracy is required
  - nuclear statistical uncertainty
  - nuclear systematic uncertainty
  - higher-order EM operators

- uncertainty improvement with δ_{TPE} in μ^2H

Hernandez, Ekström, Nevo Dinur, CJ, Bacca, Barnea, PLB 788 (2018) 377
Hernandez, CJ, Bacca, Barnea, Nevo-Dinur, PRC 100 (2019) 064315
Nevo-Dinur, Hernandez, Bacca, Barnea, CJ, Pastore, Piarulli, Wiringa, PRC 99 (2019) 034004
Emmons, CJ*, Platter, J. Phys. G 48, 035101 (2021)

Nuclear statistical error

- (statistically) optimized chiral potential
  Ekström *et al.*, PRL (2013), JPG (2015); Carlsson *et al.*, PRX (2016)

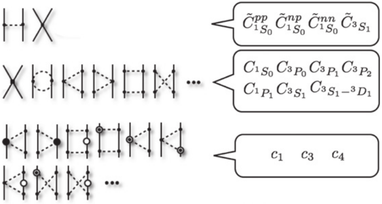

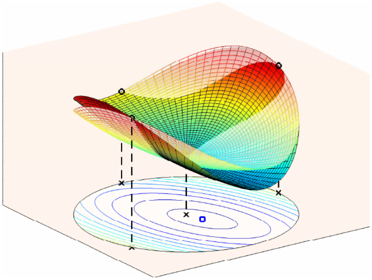

$\min(\chi^2)$

Estimate statistical errors

- covariance of low-energy constants $\mathrm{Cov}(c_i, c_j)$
- covariance of observables

$$\mathrm{Cov}(A,B) = \frac{\partial A}{\partial c_i} \mathrm{Cov}(c_i, c_j) \frac{\partial B}{\partial c_j}$$

- statistical error $\sigma_A^2 = \mathrm{Cov}(A, A)$
- $\sigma_{\mathrm{stat}}(\delta^A_{\mathrm{TPE}}) = 0.05\%$

Hernandez, Ekström, Nevo Dinur, CJ, Bacca, Barnea, PLB 788 (2018) 377

Correlations among ^{2}H observables

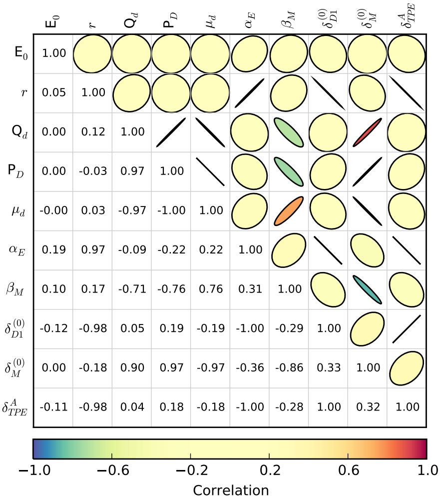

	E_0	r	Q_d	P_D	μ_d	α_E	β_M	$\delta_{D1}^{(0)}$	$\delta_M^{(0)}$	δ_{TPE}^{A}
E_0	1.00									
r	0.05	1.00								
Q_d	0.00	0.12	1.00							
P_D	0.00	-0.03	0.97	1.00						
μ_d	-0.00	0.03	-0.97	-1.00	1.00					
α_E	0.19	0.97	-0.09	-0.22	0.22	1.00				
β_M	0.10	0.17	-0.71	-0.76	0.76	0.31	1.00			
$\delta_{D1}^{(0)}$	-0.12	-0.98	0.05	0.19	-0.19	-1.00	-0.29	1.00		
$\delta_M^{(0)}$	0.00	-0.18	0.90	0.97	-0.97	-0.36	-0.86	0.33	1.00	
δ_{TPE}^{A}	-0.11	-0.98	0.04	0.18	-0.18	-1.00	-0.28	1.00	0.32	1.00

Correlation $\rho(A,B) = \frac{\mathrm{Cov}(A,B)}{\sigma_A \sigma_B}$

strong correlation groups

- group 1: E_0
- group 2: r_d, α_D, δ_{TPE}
- group 3: Q_d, μ_d, β_M

Hernandez, Ekström, Nevo Dinur, CJ, Bacca, Barnea, PLB 788 (2018) 377

Nuclear systematic error

- expansion truncation error: $(Q/\Lambda_b)^{n+2}\max\{c_i\}$
  $Q \sim \max(p, m_\pi)$; $\Lambda_b \sim 600\mathrm{MeV}$ Epelbaum et al. EPJA '15; Furnstahl et al. PRC '15
- fitting truncation error: $T_{\rm lab}$
- Cutoff (Λ) dependence

$\mathrm{N}^2\mathrm{LO}_{\rm sim}$: $\sigma_{\rm sys}(\delta^A_{\rm TPE})$

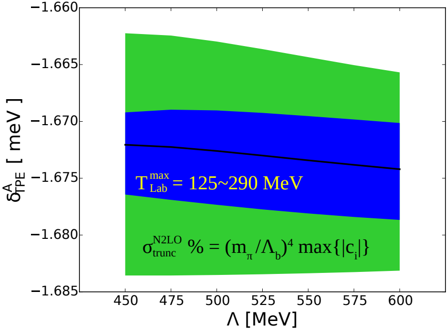

$\mathrm{N}^k\mathrm{LO}_{\rm EKM}$ Epelbaum, Krebs, Meißner, PRL '15
$\mathrm{N}^k\mathrm{LO}_{\rm EMN}$ Entem, Machleidt, Nosyk, PRC '17
$\mathrm{N}^k\mathrm{LO}_{\rm sim}$ Carlsson *et al.*, PRX '16

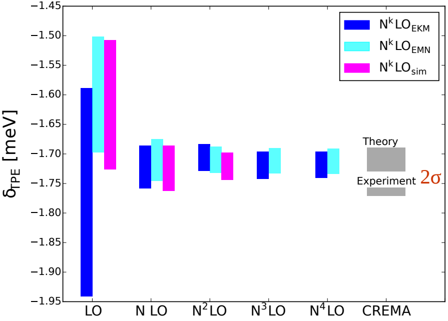

Result is consistent with previous work, ^{2}H radius puzzle remains!

Hernandez, Ekström, Nevo Dinur, CJ, Bacca, Barnea, Phys. Lett. B 788 (2018) 377

Higher-order EM operators

- higher-order currents are constructed from chiral EFT
- relativistic and meson-exchange currents (RC+MEC)

$$\mathbf{j} = \sum_{n=-2}^{+1} \mathbf{j}^{(n)}, \quad \rho = \sum_{n=-3}^{+1} \rho^{(n)}$$

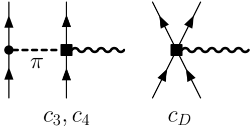

Pastore *et al.*, PRC '08,'09,'11; Kölling *et al.*, PRC '09,'11

		r_d [fm]	Q_d [fm^2]
N3LO	Impulse Approx	1.976	0.2750
	+RC+MEC	1.976	0.2851
AV18	Impulse Approx	1.969	0.2697
	+RC+MEC	1.969	0.2806
Experiment		1.9751(8)	0.28578(3)

Piarulli *et al.* PRC '13

Higher-order EM operators

- higher-order currents are constructed from chiral EFT
- relativistic and meson-exchange currents (RC+MEC)

$$\mathbf{j} = \sum_{n=-2}^{+1} \mathbf{j}^{(n)}, \quad \rho = \sum_{n=-3}^{+1} \rho^{(n)}$$

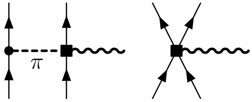

Pastore *et al.*, PRC '08,'09,'11; Kölling *et al.*, PRC '09,'11

		r_d [fm]	Q_d [fm^2]
N3LO	Impulse Approx	1.976	0.2750
	+RC+MEC	1.976	0.2851
AV18	Impulse Approx	1.969	0.2697
	+RC+MEC	1.969	0.2806
Experiment		1.9751(8)	0.28578(3)

Piarulli *et al.* PRC '13

- Test RC+MEC contributions to δ_{Zem} & other EM moments

RC+MEC contributions to EM moments in ^{2}H

Method	R_E [fm]	$\langle R_E^3 \rangle_{(2)}$ [fm^3]	$\langle R_E^4 \rangle$ [fm^4]	R_Z [fm]	R_M [fm]	μ [μ_N]
IA	1.953(1)	27.56(20)	32.5(1.3)	2.598(1)	2.103(1)	-1.757(1)
IA+RC	1.975(1)	28.44(20)	33.6(1.3)	2.621(1)	2.116(1)	-1.737(1)
TOT	1.979(1)(10)	28.58(66)(13)	33.8(1.5)(2)	2.539(3)(19)	1.991(1)(31)	-2.093(1)(55)
Exp.	1.973(14)	28.15(70)	32.9(1.60)	2.528(16)	1.976(47)	-2.127

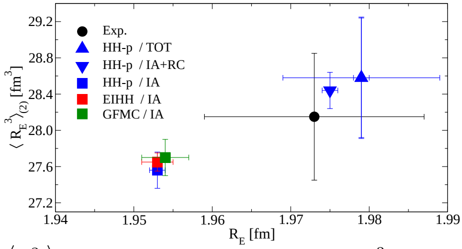

$$\left\langle R_E^3 \right\rangle_{(2)} = \iint d\boldsymbol{r} d\boldsymbol{r}' \rho_E(\boldsymbol{r}) \rho_E(\boldsymbol{r}') \left|\boldsymbol{r} - \boldsymbol{r}'\right|^3$$

electric Zemach moment

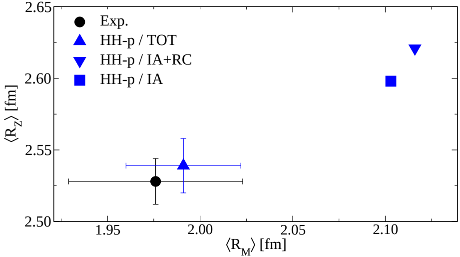

$$R_Z = \iint d\boldsymbol{r} d\boldsymbol{r}' \rho_E(\boldsymbol{r}) \rho_M(\boldsymbol{r}') \left|\boldsymbol{r} - \boldsymbol{r}'\right|$$

magnetic Zemach moment

Nevo-Dinur, Hernandez, Bacca, Barnea, CJ, Pastore, Piarulli, Wiringa, PRC 99, 034004 (2019)

Nuclear EM moments in ^{3}He

calculations of EM moments of ^{3}He (Impulse Approx; AV18+UIX)

Method	R_E [fm]	$\langle R_E^3 \rangle_{(2)}$ [fm^3]	$\langle R_E^4 \rangle$ [fm^4]	$\langle R_Z \rangle$ [fm]	R_M [fm]	μ [μ_N]
VMC	1.956(1)	27.8(1)	33.5(1)	2.58(1)	2.000(1)	$-1.774(1)$
GFMC	1.954(3)	27.7(2)	33.7(4)	2.60(1)	1.989(8)	$-1.747(2)$
HH-p	1.953(1)	27.56(20)	32.5(1.3)	2.598(1)	2.103(1)	$-1.757(1)$
EIHH	1.953(2)	27.65(10)	33.8(2)	-	-	$-1.758(1)$
Exp.	1.973(14)	28.15(70)	32.9(1.60)	2.528(16)	1.976(47)	-2.127

- theory (ab-initio): Nevo-Dinur, Hernandez, Bacca, Barnea, CJ, Pastore, Piarulli, Wiringa, PRC 99, 034004 (2019)
- experiment (scattering data): Sick, PRC 90, 064002 (2014)

- MEC+RC will be included in future calculations

Hyperfine splittings (HFS) in muonic atoms

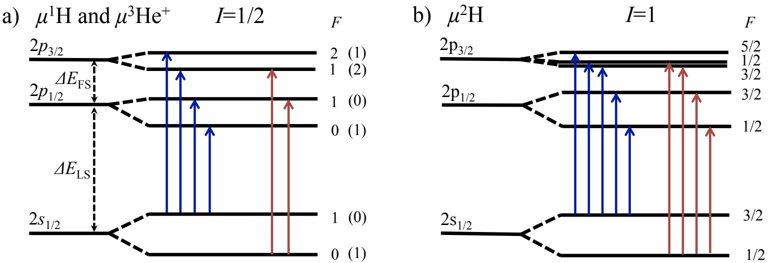

$\Longrightarrow$ determine nuclear Zemach radius R_Z

$$R_Z = \iint d\boldsymbol{r} d\boldsymbol{r}' \rho_E(\boldsymbol{r}) \rho_M(\boldsymbol{r}') \left|\boldsymbol{r} - \boldsymbol{r}'\right|$$

Hyperfine splittings (HFS) in ^{6,7}Li atoms

- R_z discrepancies in spectroscopy and scattering experiments
- Is polarizability effect underestimated in lithium hyperfine structures?

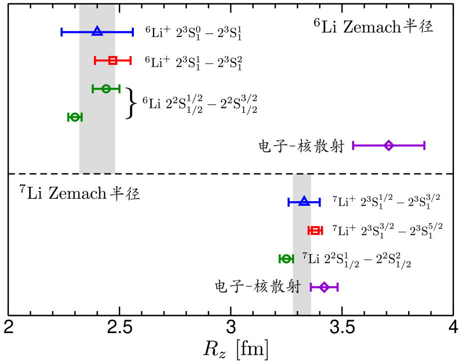

Two-photon contributions to HFS

- We plan to study 2γ exchange contributions to HFS
- From Friar, Payne, Phys. Rev. C 72, 014002 (2005):

$$\delta_{\mathrm{TPE}} = (4\pi\alpha)^2 \left|\phi_n(0)\right|^2 \int \frac{d^4q}{(2\pi)^4} \frac{(\vec{\sigma}\times\vec{q})^m \left[\mathcal{T}^{m0}(q,-q) - \mathcal{T}^{0m}(q,-q)\right]}{\left(q^2+i\epsilon\right)^2 \left(q^2 - 2m_\mu q_0 + i\epsilon\right)}$$

- nuclear Compton tensor

$\mathcal{T}_{0m} =$ 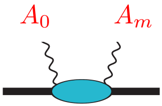

  - elastic part: contains contribution from R_Z
  - inelastic part: polarizability
    - dominated by M1/E2 excitation
    - magnetic polarizability plays an significant role
    - meson-exchange current is important

Summary

- electron scattering and spectroscopy
  - brings nuclear structure investigation to precision levels
  - many puzzles remain to be understood
- Lamb shifts in muonic atoms
  - raise interesting questions about lepton symmetry
  - nuclear polarizability effects connect nuclear structures to atomic spectroscopy
- Ab initio calculations of $\delta_{\rm pol}$
  - We obtained $\delta_{\rm pol}$ in $\mu^{2,3}$H, $\mu^{3,4}$He$^+$ with percentage accuracy
  - Results are more accurate than those from photoabsorption data
- Further improvement in theoretical accuracy
  - improve accuracy in nuclear models
  - improve accuracy in photon operators
  - pionless EFT provides an alternative uncertainty estimates
- HFS in light electronic/muonic atoms
  - nuclear magnetic distribution
  - 2γ contributions to HFS